AN EXPERIMENT TO MEASURE THE MODULATION TRANSFER FUNCTION OF THE ATMOSPHERE IN THE MARINE BOUNDARY LAYER

Marion Romaine Alexander

NAVAL POSTGRADUATE SCHOOL
Monterey, California

THESIS

AN EXPERIMENT TO MEASURE THE MODULATION TRANSFER FUNCTION OF THE ATMOSPHERE IN THE MARINE BOUNDARY LAYER

by

Marion Romaine Alexander, Jr.

June 1974

Thesis Advisor: E. C. Crittenden, Jr.

UNCLASSIFIED

SECURITY CLASSIFICATION OF THIS PAGE *(When Data Entered)*

REPORT DOCUMENTATION PAGE		READ INSTRUCTIONS BEFORE COMPLETING FORM
1. REPORT NUMBER	2. GOVT ACCESSION NO.	3. RECIPIENT'S CATALOG NUMBER
4. TITLE *(and Subtitle)* An Experiment to Measure the Modulation Transfer Function of the Atmosphere in the Marine Boundary Layer		5. TYPE OF REPORT & PERIOD COVERED Master's Thesis June 1974 6. PERFORMING ORG. REPORT NUMBER
7. AUTHOR(s) Marion Romaine Alexander, Jr.		8. CONTRACT OR GRANT NUMBER(s)
9. PERFORMING ORGANIZATION NAME AND ADDRESS Naval Postgraduate School Monterey, California 93940		10. PROGRAM ELEMENT, PROJECT, TASK AREA & WORK UNIT NUMBERS
11. CONTROLLING OFFICE NAME AND ADDRESS Naval Postgraduate School Monterey, California 93940		12. REPORT DATE June 1974 13. NUMBER OF PAGES 66
14. MONITORING AGENCY NAME & ADDRESS*(if different from Controlling Office)* Naval Postgraduate School Monterey, California 93940		15. SECURITY CLASS. *(of this report)* Unclassified 15a. DECLASSIFICATION/DOWNGRADING SCHEDULE

16. DISTRIBUTION STATEMENT *(of this Report)*

Approved for public release; distribution unlimited.

17. DISTRIBUTION STATEMENT *(of the abstract entered in Block 20, if different from Report)*

18. SUPPLEMENTARY NOTES

19. KEY WORDS *(Continue on reverse side if necessary and identify by block number)*

Laser Propagation
Scintillation
Marine Boundary Layer
Modulation Transfer Function

20. ABSTRACT *(Continue on reverse side if necessary and identify by block number)*

A system to measure the modulation transfer function of the atmosphere over the ocean has been designed, constructed, and tested. The apparatus employs a high resolution scanning telescope with the capability for use in a broad range of visual and infrared wavelengths. Two successful trials were conducted with a gyro-stabilized 6328 A laser mounted on

DD FORM 1 JAN 73 1473 EDITION OF 1 NOV 65 IS OBSOLETE
S/N 0102-014-6601 | 1

UNCLASSIFIED

SECURITY CLASSIFICATION OF THIS PAGE *(When Data Entered)*

Block #20 continued

board the R. V. ACANIA. The propagation path was approximately 1km over open water from the ACANIA to Point Pinos. Two more successful trials were conducted with a 6328 A laser and a 10.6μ laser propagating simultaneously from shore to shore across 4km of the southern end of Monterey Bay. Data was processed using fast Fourier transformation methods. The MTF of the atmosphere for 6328 A light was measured.

An Experiment to Measure the Modulation Transfer Function of the Atmosphere in the Marine Boundary Layer

by

Marion Romaine Alexander, Jr.
Lieutenant Commander, United States Navy
B.S., United States Naval Academy, 1964

Submitted in partial fulfillment of the requirements for the degree

MASTER OF SCIENCE IN PHYSICS

from the

NAVAL POSTGRADUATE SCHOOL
June 1974

ABSTRACT

A system to measure the modulation transfer function of the atmosphere over the ocean has been designed, constructed, and tested. The apparatus employs a high resolution scanning telescope with the capability for use in a broad range of visual and infrared wavelengths. Two successful trials were conducted with a gyro-stabilized 6328 Å laser mounted on board the R. V. ACANIA. The propagation path was approximately 1km over open water from the ACANIA to Point Pinos. Two more successful trials were conducted with a 6328 Å laser and a 10.6μ laser propagating simultaneously from shore to shore across 4km of the southern end of Monterey Bay. Data was processed using fast Fourier transform methods. The MTF of the atmosphere for 6328 Å light was measured.

TABLE OF CONTENTS

LIST OF DRAWINGS

I. INTRODUCTION

With the increasing applications of electro-optic devices it is important to thoroughly understand the effects that the atmosphere has on optical transmission.

A. ATMOSPHERIC EFFECTS

Atmospheric effects on optical transmission may be classified into two general categories. The first is seen only when high power laser beams are utilized. When significant amounts of beam energy are absorbed by the atmosphere, the atmosphere becomes heated. This results in a change of density and leads to a change of refractive index. The effect is more pronounced near the center of the beam than at the edges. As a result, the atmosphere acts like a diverging lens. If the air is moving, or the beam is moving with respect to the air, then the effect also causes a bending of the beam into the relative wind. While the first category effect is caused by laser induced atmospheric changes, the second category effects are caused by normal meteorological phenomena which are independent of the laser beam and may be observed for either high or low power lasers. These effects are absorption, scattering, scintillation, beam spread, beam wander, and the consequent reduction in modulation transfer function (MTF). Absorption is caused primarily by carbon dioxide and water vapor; scattering by aerosols and particulates. Scintillation, beam wander, and beam

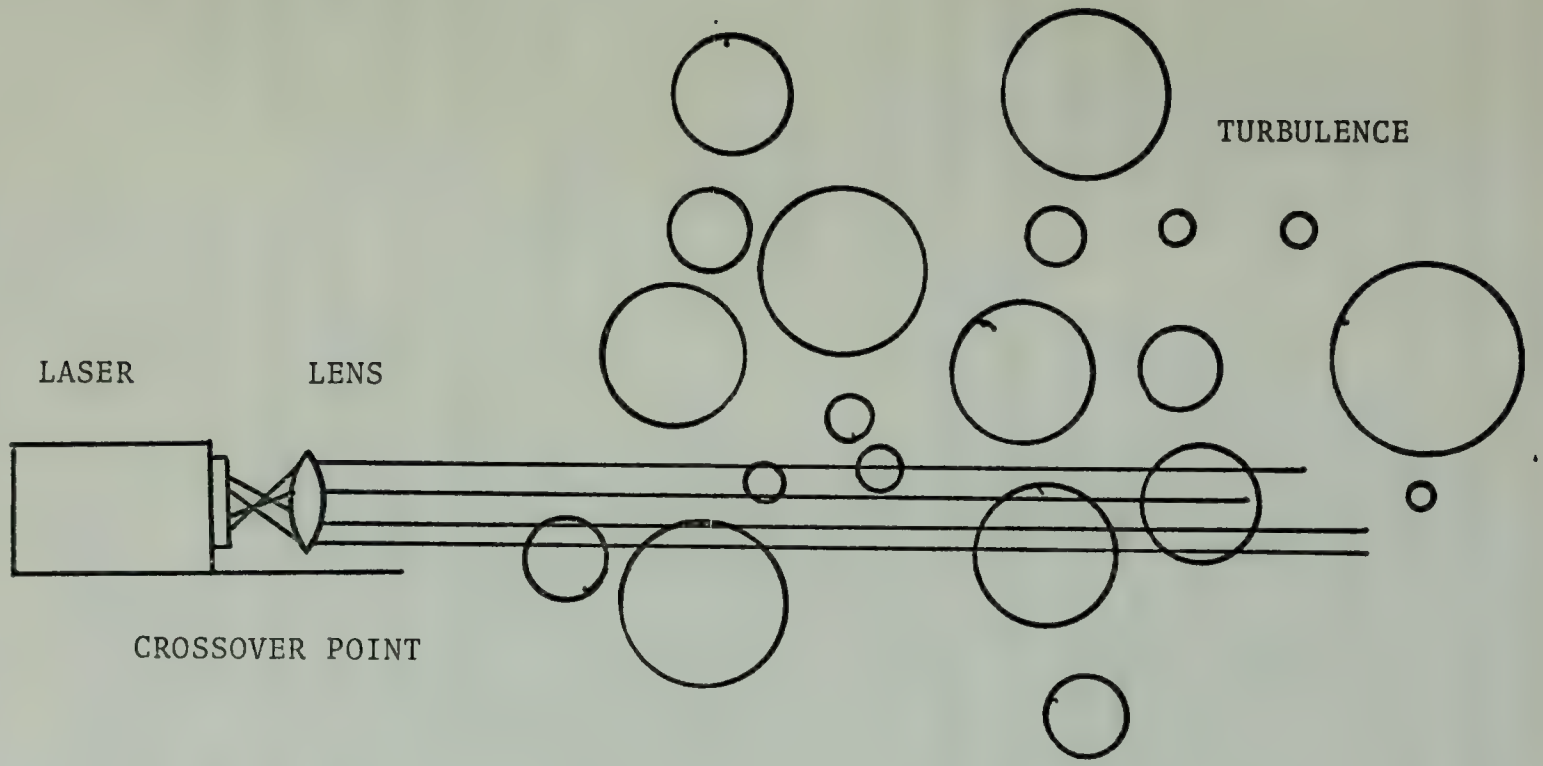

Figure 1. Propagation Through Turbulence.

spread are caused by many random, non-uniform changes of refractive index along the transmission path of the beam. These refractive index changes are the result of variations of temperature and humidity caused by turbulence.

The measurement of beam wander and beam spread and its equivalent, the modulation transfer function of the atmosphere, will be dealt with in this thesis. Specifically, experiments and equipment to measure these values in the atmosphere, directly over the ocean surface will be described. The experiments were conducted at two wavelengths; 6328 Angstroms and 10.6 microns.

B. MATHEMATICAL DESCRIPTION

For 5000 Å light the refractive index of the atmosphere may be described by

$$n = 1 + 80\times10^{-6}\,\frac{P}{T} + 41\times10^{-6}\,\frac{m}{760}$$

where T is measured in °k. The absolute pressure, P, and the partial pressure of water vapor, m, are measured in millibars [Ref. 1]. The constants differ slightly for different wavelengths. In the atmosphere, relative temperature fluctuations are much stronger than relative temperature or humidity fluctuations [Ref. 2,3]. Thus refractive index changes should be most directly related to the temperature fluctuations [Ref. 2].

Refractive index gradients cause bending of the laser beam. If the atmosphere is turbulent and the beam diameter is of the same order of magnitude as the distance in which

significant refractive index fluctuations occur, the bending of the beam may be very complicated, because different parts of the beam will pass through regions of different refractive index. This complicated bending results in a change of cross-sectional shape and area (beam spread), propagational direction (beam wander, and intensity (scintillation) [Ref. 4]. Under normal meteorological conditions near the earth's surface, significant variations occur over lengths of the order of millimeters to meters [Ref. 5]. This is small enough to significantly affect beams of all sizes. There may be as many as 10^3 to 10^6 of these variations or vortex cells in a propagation path of 1km.

1. Beam Wander and Beam Spread

Clearly a solution of the motion of the beam under these circumstances is impossible unless a statistical model is used to describe the effects of atmospheric turbulence on the beam. Tatarski [Ref. 2] pioneered this formalism. His model and all other successful models require the assumption that the transverse refractive index fluctuates randomly. The refractive index structure constant, C_N is defined as follows:

$$C_N \equiv [D_n(\bar{r})]^{\frac{1}{2}} r^{-1/3}, \quad \ell_o < r < L_o \tag{1}$$

where

$$D_n = \langle [n(\bar{R}) - n(\bar{R} + \bar{r})]^2 \rangle \tag{2}$$

$\bar{r}$ is a vector between two points in the transmitter aperture

$\bar{R}$ is a vector to any point within the common area of two circles with centers at the end points of $\bar{r}$

ℓ_o is the smallest turbulence scale present

L_o is the largest turbulence scale present

<> indicates an ensemble average over all realizations of the atmosphere for fixed meteorological conditions.

C_N may be determined through either scintillation or micro-meteorological measurements. At 6328 Å

$$C_N \equiv 79 \frac{P}{T^2} x10^{-6} C_T$$

where P is measured in millibars and T in °k [Ref. 10]. The temperature structure constant, C_T, is the root mean square temperature difference between two points separated by a distance r, divided by the cube root of the distance.

$$C_T = [\overline{(T_1 - T_2)^2}]^{\frac{1}{2}} r^{-1/3}.$$

Optical measurements by Haagensen [Ref. 6] and Schroeder [Ref. 7] correlate strongly with C_N determined simultaneously from meteorological measurements taken near the midpoint of the propagation path.

Tatarski showed that a power spectrum based on refractive index fluctuations is proportional to the velocity spectrum of the turbulence. Strohbehn [Ref. 5] developed an expression for the refractive index power spectrum, $\Phi_n(k)$ based on Tatarski's findings and the assumption of isotropy which allows equations (1) and (2) to be converted into scalar equations.

$$\Phi_n(k) = 0.033C_N \exp[-k^2/k_m^2]k_o^{-11/3}(1+k^2/k_o)^{-11/6} \quad (3)$$

where

k = spatial wave number

$k_m = 5.92/\ell_o$

$k_o = 2\pi/L_o$.

A wave structure function ($D(r,z)$) has been developed from $\Phi_n(k)$ [Ref. 2, 5, 8].

$$D(r,z) = 4\pi k_o^2 z \int_o^1 dy \int dk\, \Phi_n(k)(1-\exp[i\bar{k}\cdot\bar{r}(1-y)]) \quad (4)$$

where

z = distance along the beam from the transmitter

k_o = optical frequency wave number.

$D(r,z)$ may be inserted into the Fresnel-Kirchoff integral to give the time average irradiance in the receiver plane [Ref. 8].

$$I(\bar{w}) = (k_o^2/2\pi z)\int d\bar{r}\, F(\bar{r},z)\exp[\tfrac{1}{2}D(r,z)]$$

$$\exp[-ik\bar{w}\cdot\bar{r}/z] \quad (5)$$

where

$\bar{w}$ = position in the receiver plane

$F(\bar{r},z)$ = aperture function projected through the distance

$= \int \partial Ru(R+\tfrac{1}{2}r)^*(R-\frac{1}{2r})\exp[ik_o\bar{R}\cdot\bar{r}/z]$

u = amplitude of the radiation in the aperture.

Several approximations have been made to (5) which give expressions for beam wander or beam spread in terms of C_N, z, and either k_o or ℓ_o [Ref. 6]. According to Dowling and Livingston beam wander ϕ^2 is given by

$$\phi^2 = 32\pi^2 \, zF/3L_1$$

where

$$L_1 = 1/[(\tfrac{1}{2})x0.033C_N^2 \, k_m^{-1/3}].$$

F is a complicated function of transmitter aperture and turbulence which is independent of z, k_o and C_N [Ref. 8, 11].

Dowling and Livingston utilized the well known property of a Gaussian distribution to obtain

$$\theta' = \theta^2 + \phi^2$$

where

θ = short term average beam width expressed as the angle in radians from the transmitter subtended by the $1/e^2$ power distribution width in the focal plane of the beam

θ' = long term average beam width expressed in the same terms [Ref. 8].

Therefore, to obtain beam spread or MTF, the beam wander must be removed.

Chiba gives a graph of standard deviation of beam motion, σ_x, versus path length L for several values of C_N which shows the increase of beam wander with turbulence.

2. Modulation Transfer Function

The modulation, M, of a signal is defined

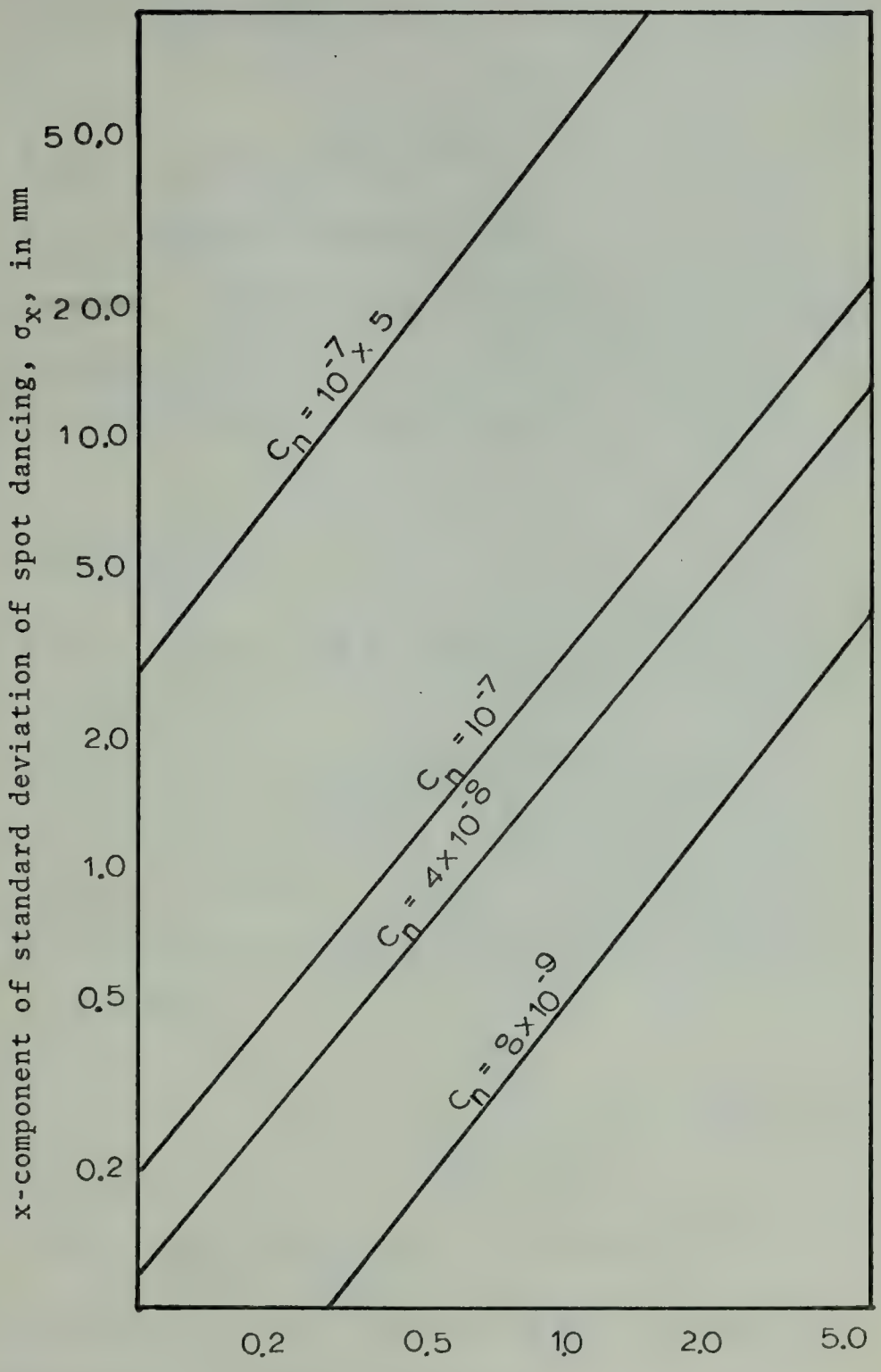

Figure 2. Path Length, L, in km.

$$M = \frac{H_{max} - H_{min}}{H_{max} + H_{min}}$$

where

H_{max} = maximum signal amplitude

H_{min} = minimum signal amplitude.

Thus the modulation is the ratio of the amplitude variation to twice its average amplitude. The modulation transfer function, MTF, is the ratio of output modulation to input modulation.

$$MTF = \frac{M_{out}}{M_{in}} .$$

The MTF is a measure of the optical system's ability to transmit information.

The MTF may also be defined through use of the properties of the Fourier transform. A point source located at infinity imaged by a mirror, produces a diffraction pattern which is the Fourier transform of the mirror aperture.

$$h = F\{p\}$$

where

h = point spread function or impulse response

p = pupil function of aperture

$F\{\}$ = implies the Fourier transform of the quantity in braces.

The image function, U_i, is the convolution of the object function with the point spread function.

$$U_i = h * U_o .$$

The angular spectrum, A_o, is the Fourier transform of the object function.

$$A_o = \mathcal{F}\{U_o\}$$

$$A_i = \mathcal{F}\{U_i\}$$

$$U_i = h * U_o$$

$$\mathcal{F}\{U_i\} = \mathcal{F}\{h * U_o\}$$

$$A_i = \mathcal{F}\{h\}\ \mathcal{F}\{U_o\}$$

$$A_i = \mathcal{F}\{\mathcal{F}\{P\}\}\ A_o$$

$$A_i = -P\ A_o$$

where the negative sign implies an inverted image.

$$P = \frac{-A_i}{A_o} .$$

For coherent light the absolute values of P is defined as the MTF.

$$MTF = P = \left|\frac{A_i}{A_o}\right| .$$

The MTF for a coherent system is constant from zero spatial frequency to a cutoff spatial frequency ν_c.

$$\nu_c = \frac{kd}{2f}$$

where

k = wave number

d = aperture diameter

f = focal length.

For a non-coherent system

$$I_i = |h|^2 * I_o$$

where

I_o = object intensity

I_i = image intensity

$$I_i = |\mathcal{F}\{P\}|^2 * I_o$$

$$\mathcal{F}\{P(x) * P(-x)\} * I_o.$$

Taking the Fourier transform of both sides,

$$\mathcal{F}\{I_i\} = \mathcal{F}\{\mathcal{F}\{P(x) * P(-x)\} * I_o\}$$

and applying the convolution theorem,

$$\mathcal{F}\{I_i\} = \mathcal{F}\{\mathcal{F}\{P(x) * P(-x)\}\}\mathcal{F}\{I_o\}$$

$$\mathcal{F}\{I_i\} = -[P(x) * P(-x)]\mathcal{F}\{I_o\}$$

$$G_i = -P(x) * P(-x)\ G_o$$

where

$G_i = \mathcal{F}\{I_i\}$

$G_o = \mathcal{F}\{I_o\}$

$$\frac{G_i}{G_o} = -P(x) * P(x) = \text{MTF}.$$

The MTF of a non-coherent system is the autocorrelation of the pupil function. The MTF of a circular aperture may be determined by a geometrical solution of the autocorrelation. It is the area of the overlap of the circle, D_o, as it convolves with itself, divided by the area of the aperture D.

$$MTF = \frac{D_o}{D} .$$

Obviously the MTF varies from a value of one at zero spatial frequency, where the area of overlap is equal to the area of the aperture, to a value of zero where there is no overlap. The cutoff spatial frequency ν_{nc} is twice the cutoff spatial frequency ν_c.

The transfer function for a system is equal to the product of the transfer functions of the individual components.

$$H(\omega) = H_1(\omega)\ H_2(\omega)\ H_3(\omega)....H_n(\omega).$$

To find the transfer function of any one component it is necessary to know the transfer functions of the system and the other components or the product of the other components. The transfer function of the desired component is then found by a simple quotient.

$$H_1(\omega) = \frac{H(\omega)}{H_2(\omega)H_3(\omega)....H_n(\omega)} .$$

Since H and $H_1, H_2, ...H_n$ are all function of ω it is necessary to divide point by point to find $H(\omega)$.

For a coherent system the transfer function is the MTF. For a non-coherent system the MTF is the autocorrelation of the transfer function. If the MTF of a system is known, the MTF of the atmosphere can be calculated by this method.

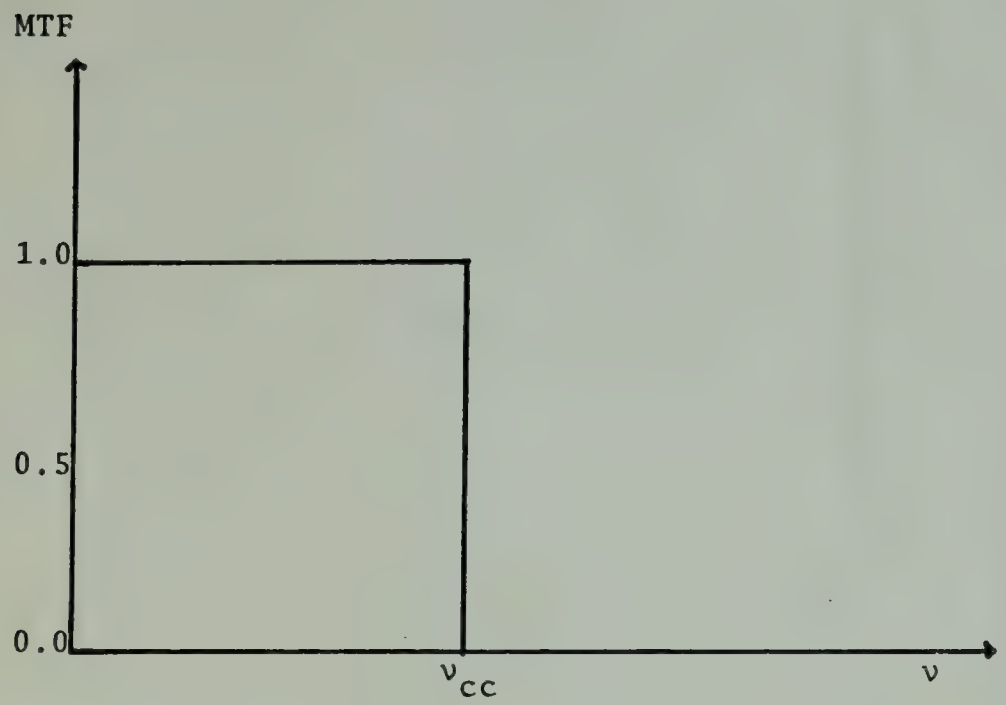

Figure 3. MTF of a Circular Aperture for Coherent Light.

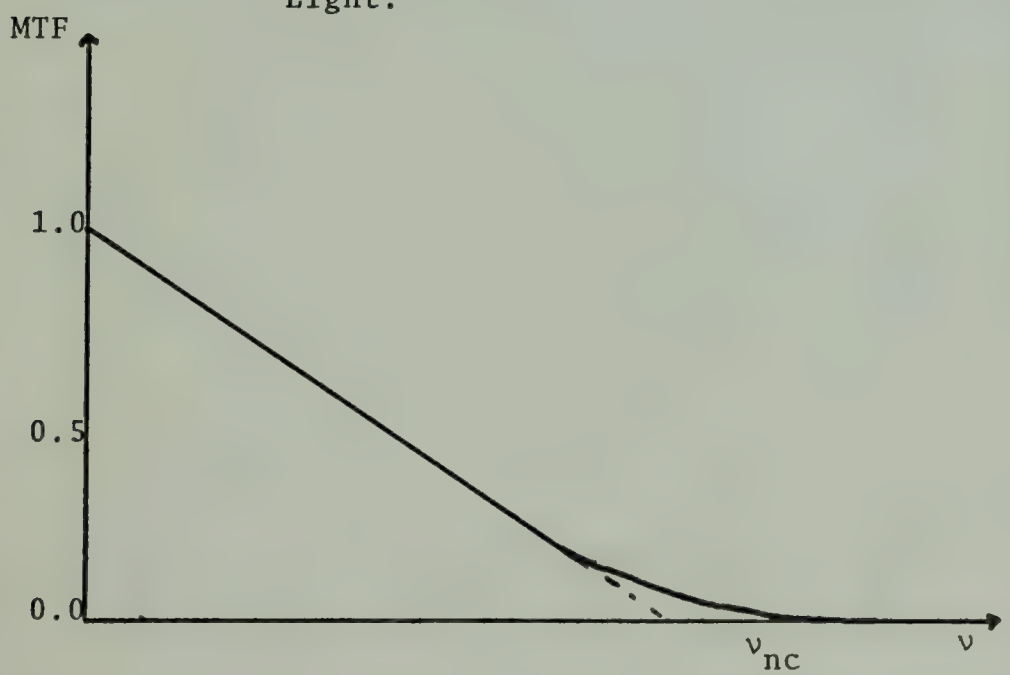

Figure 4. MTF of a Circular Aperture for Non-Coherent Light.

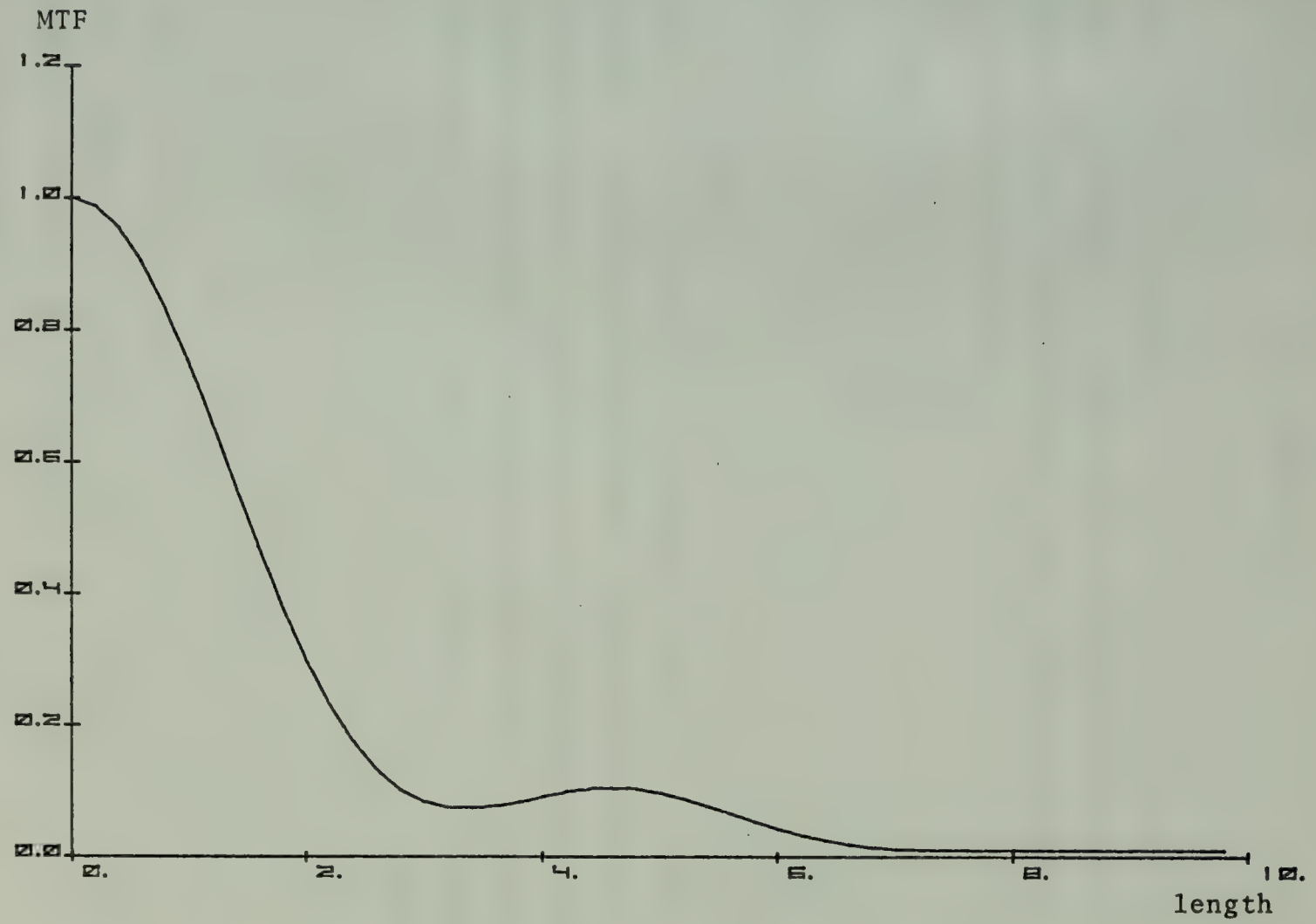

Figure 5. MTF of Scanning Telescope.

II. APPARATUS

As noted by Beal, no previous measurements of beam wander and beam spread or MTF had been conducted over the ocean. The conduct of the experiment over water imposes several significant constraints which are not applicable to over land measurements.

A. DESIGN CONSIDERATIONS

The two primary constraints are portability and tracking ability. The system must be portable for several reasons. First, because it is still in an evolutionary stage components are being replaced or modified constantly. After each change is completed, the component and system must be thoroughly tested. Tests are usually conducted indoors in the 400 foot basement corridor of Spanagel Hall at the Naval Postgraduate School. Second, the system must be transported to a site which is accessible to the ocean and has acceptable meteorological conditions. Third, while the experiment has evolved from indoor measurements to over water with fixed end points, to ship to shore, the ultimate goal is ship to ship measurements. Some of the components presently in use may eventually go to sea. Clearly, the system must be capable of tracking a moving target.

1. Precision

References 8 and 10 indicated that beam wander measurements over land were of the order of 100 microradians

for path lengths in the kilometer range. Beal measured beam wander down to 4.6 microradians and beam spread down to 2.0 microradians over water. Measurements of this magnitude require high quality optics and data reduction methods capable of removing the motion of the source from the beam motion and measuring MTF in the presence of motion.

2. Magnification

Because the length of the slit is limited, system magnification must be such that the motion of the source mounted on a ship at sea does not cause its image to move on and off the detector.

3. Wavelength Capability

There are at least three wavelengths of considerable interest: 6328 Angstroms in the visible range and 3.8 and 10.6 microns in the infrared. The system should be capable of handling all three with at least two simultaneously. To handle visible and infrared simultaneously, reflective optics must be used throughout.

B. EVOLUTION

The first telescope used in this experiment was a Cassegranian with a 9.2 cm parabolic primary mirror which had a 92.4 cm focal length. It utilized a rotating eight sided prism for scanning. The second telescope was a Newtonian with a 25.4 cm spherical primary mirror which had a 204.5 cm focal length. It utilized a Galvanometer movement driven by an oscillator for scanning. Hildebrand [Ref. 12] and Beal report descriptions of both systems.

C. PRESENT CONFIGURATION

The current system is essentially the same that Beal used. The scanning system has been changed and it can now be trained in azimuth and elevation.

1. Telescope Optics

The primary mirror is spherical with a 25.4 cm diameter. The larger mirror was utilized to reduce diffraction effects. It has a 204.5 cm focal length. It is mounted in a square tube which is approximately the same length as the focal length. Just before the focal plane, a flat 5x7.5 cm elliptical mirror is mounted. It is oriented 45 degrees from the telescope axis. The turning mirror obscures a 5 cm diameter circle along the telescope axis. Incoming light is reflected by the primary mirror onto the turning mirror which reflects the light onto the scanning mirror located on the top of the telescope. For objects at a range of 1km the magnification of the system is approximately 0.002. This means that source motion of 5 meters will only result in image motion of 1 cm. This is within the limits imposed by the turning mirror, scanning mirror and detector slit.

2. Scanner Unit

The galvanometer movement has been replaced by a General Scanning Inc. scanner motor. It drives a flat 2.5 cm diameter mirror which scans the image across the detector slit. The motor is designed to be driven by a ramp driver amplifier which causes the mirror to move linearly. Tests, however, indicated that the mirror was less linear than that

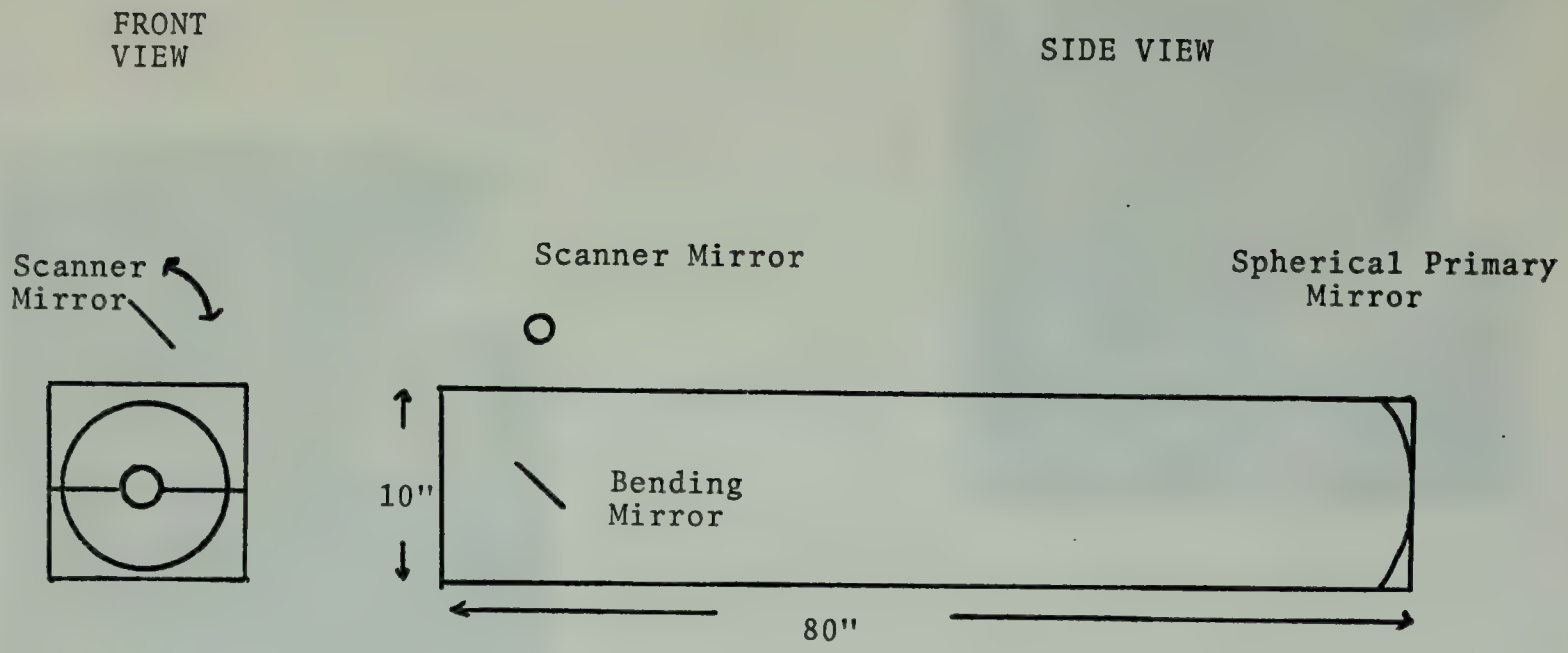

Figure 6. Telescope Optics.

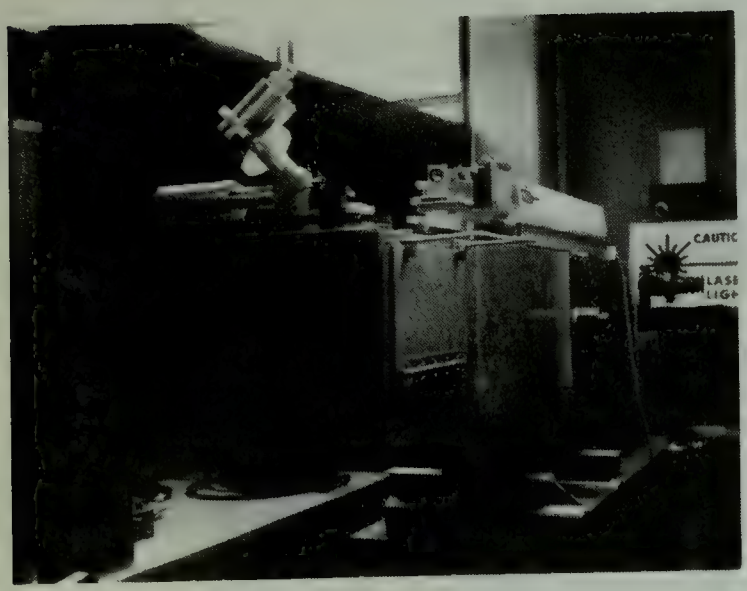

Figure 7. Telescope and Scanner.

obtained when a sinusoidal input was applied. An attempt was also made to scan with the power line current reduced by a variac but the portable generator had a bad wave form and the frequency was too high. Accordingly an oscillator is used to drive the scanner motor. The motion closely approaches linearity near the midpoint. A variable D.C. bias voltage can be applied to the scanner to provide fine steering by shifting the scan center.

3. Detector Unit

The detector unit is composed of a variable slit 1.5 cm long, a plane glass beam splitter, lenses, filters and two detectors. Visible light passes through the glass beam splitter and filter. It is focused by two lenses onto a 1 cm circular E.G.&G. Inc. SGD-444 silicon photodiode. It has been tested and found to have uniform response within 2.5 percent over its entire area [Ref. 4]. The detector is located slightly off the focal point so that the signal falling upon it is slightly misfocused. This reduces the peak signal amplitude incident on the detector and averages out some of the small non-uniform response. The infrared detector is a 2mm x 2mm square Mercury Cadmium Telluride Detector manufactured by Santa Barbara Research Center. It is located behind an IRTRAN II window and two germanium lenses. The two lens systems are designed to focus the slit image on the detectors. This avoids image motion on the detector except motion parallel to the slit which is slow.

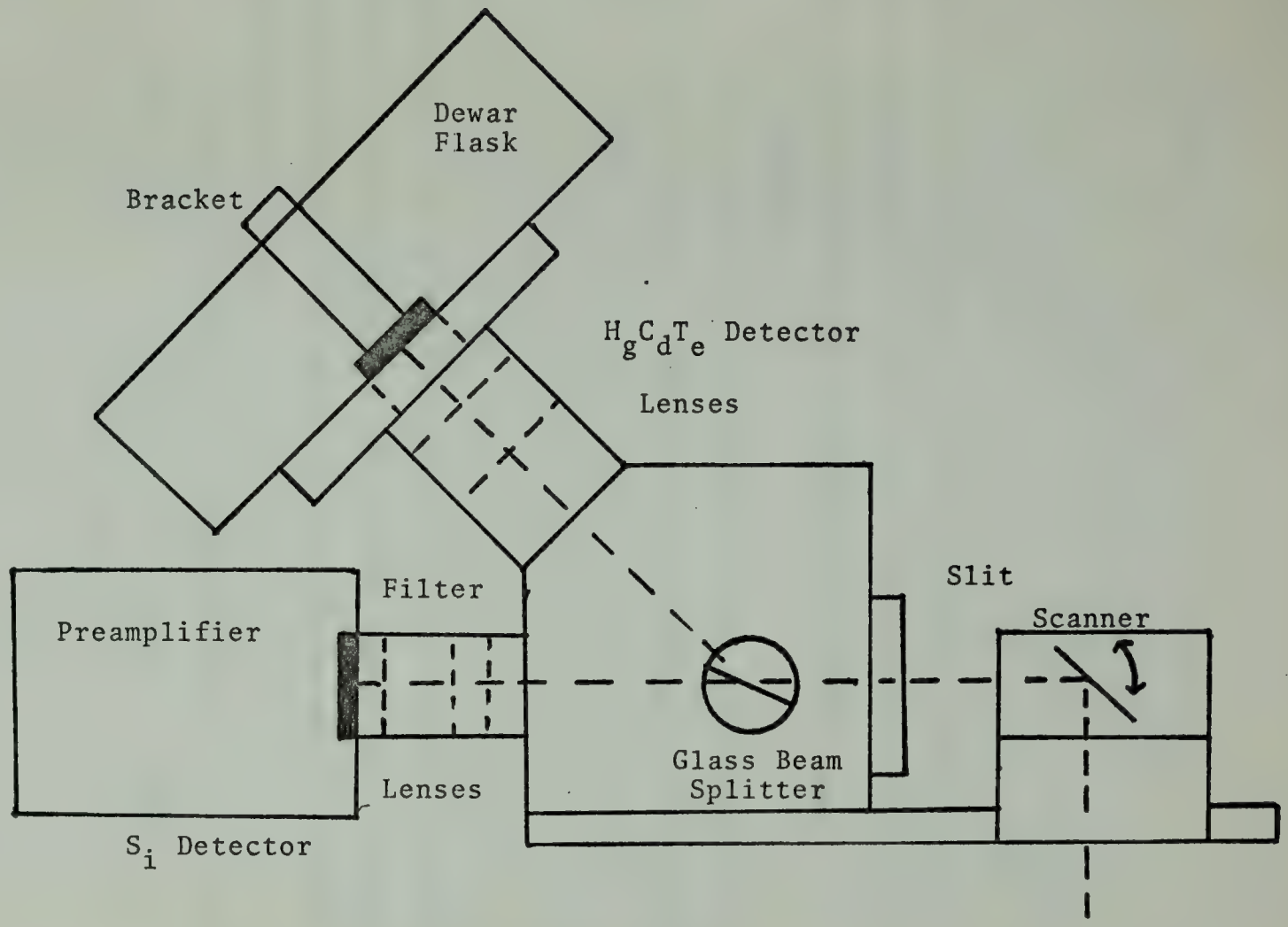

Figure 8. Scanner-Detector Unit.

The position of the scanner and detector unit along with that of the folding mirror are adjustable so that the image may be formed at the detector for object (source) distances from 100 meters to infinity. The entire scanner and detector assembly may be rotated through 90 degrees in a vertical plane so that the beam may be scanned both horizontally and vertically in its transverse plane.

4. Circuitry

The detector signals are amplified and then recorded on a Hewlett-Packard 3960E F.M. four channel instrumentation tape recorder. The recorder is operated at 15 inches per second, providing 0 to 5000 Hz frequency response at the 3 db points. The recorder also records the scanner drive signal and a voice annotation. A dual trace oscilloscope monitors the output of the two signal channels. The horizontal sweep of the oscilloscope is driven by the scanner drive signal.

Since both signals are only positive and the tape recorded records both positive and negative voltages, both signals are biased negatively, effectively doubling the signal to noise ratio. Overall, the visible detector circuit has a signal to noise ratio of 2000 to 1 and the infrared detector circuit 4×10^4 to 1.

Figure 9. System Schematic.

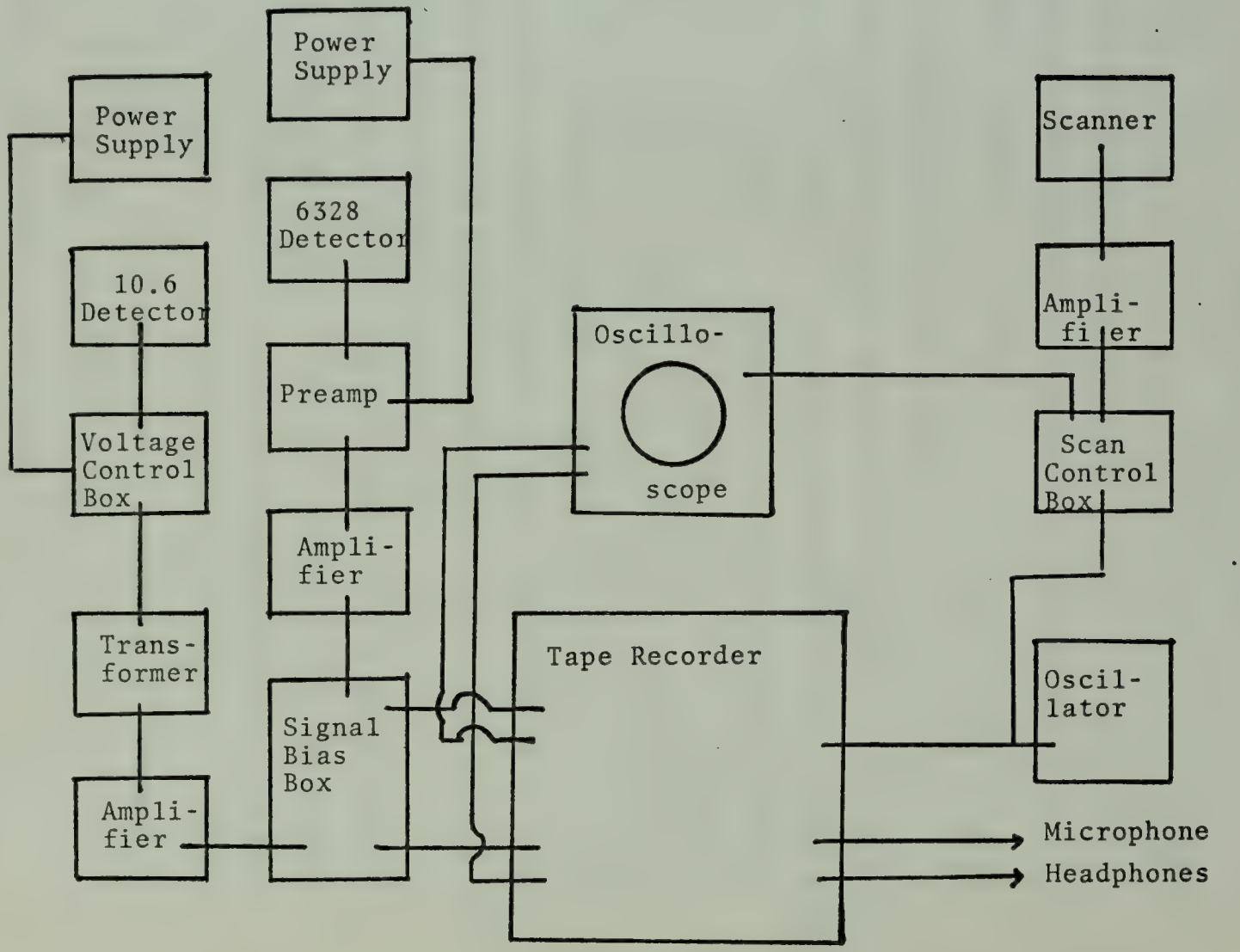

III. EXPERIMENTAL PROCEDURES

The conduct of the experiment is greatly complicated by the moving source. In a moderate sea the motion of the source on the ship, even though gyro-stabilized, is hard for the telescope to follow.

A. INITIAL TRACKING AND LOCK ON

The source is a gyro-stabilized platform, on which are mounted two lasers: a He-Ne 6328 Å and CO_2 10.6μ. The gyro system is capable of locking on to and tracking a 6328 Å signal. A He-Ne laser is mounted on the telescope to provide this signal. The entire platform is mounted on board the R. V. ACANIA, a research vessel operated by the Naval Postgraduate School. Also, on board the ACANIA are instruments to measure micrometeorological data and detectors to measure scintillation data.

The ACANIA anchors while conducting the experiment to reduce horizontal ship motion. Once the ship is in position the telescope and laser are manually pointed at the source on the ship. The telescope must continue tracking throughout the experiment. The laser beam is diverged sufficiently so that small ship motions, such as vertical motion in a moderate sea, do not have to be followed. The source then locks onto the telescope laser and tracks it. This ensures that the source is always pointed directly at the telescope and the telescope at the source.

1. Focusing

Once the source and laser are tracking each other the 6328 Å signal can be observed on the face of the detector unit slit. It must then be focused. Initial focusing is accomplished by adjusting the position of the folding mirror until the image appears to be focused on the slit face. The detector package is moved until the received signal is maximized. The focus is then checked by inserting a diffraction grating just prior to the telescope. Proper focus is taken as the position of highest resolution of the diffraction peaks.

2. Slit Width

The width of the slit governs the signal strength and resolution. The more open the slit is, the more signal strength and less signal resolution. An effective compromise has been to open the slit until the signal as viewed on the oscilloscope becomes clipped or flattened; then close the slit down until the signal amplitude is reduced to one fourth or one fifth of its flattened value. This results in sufficient signal strength and adequate signal resolution. This value must be recorded so that the same value of slit width may be used when unfolding the MTF of the telescope to determine the MTF of the atmosphere.

B. FINAL TRACKING AND DATA TAKING

Once lock-on has been achieved, the system focused, and the slit properly adjusted, data can be recorded. While

recording data, it is essential that the telescope remain totally stationary. Reliable data may be taken only when the manual tracking system is not being adjusted. Fine tracking may be accomplished by adjusting the D. C. bias voltage to the scanner mirror but this should be held to a minimum during data taking.

1. Calibration

After any equipment adjustments, the system should be calibrated. This is accomplished, using a diffraction grating with a 8.95 mm center-to-center separation. When this grating is placed directly in front of the telescope and oriented perpendicular to the scan a diffraction pattern is observed in the 6328 Å signal displayed on the oscilloscope. The distance between the diffraction peaks of the 6328 Å signal corresponds to 70.7 microradians of angular deflection.

2. Data Recording

Data is recorded on the tape recorder in short intervals (10-30 seconds) dictated by the motion of the source. The two data channels and voice channel are calibrated to record plus or minus 2.5 volts, the scan signal channel to 10.0 volts. Since the tape recorder records equally positive and negative and the two data signals are positive only, a D. C. bias signal of minus 2.5 volts is applied. This effectively increases the signal to noise ratio.

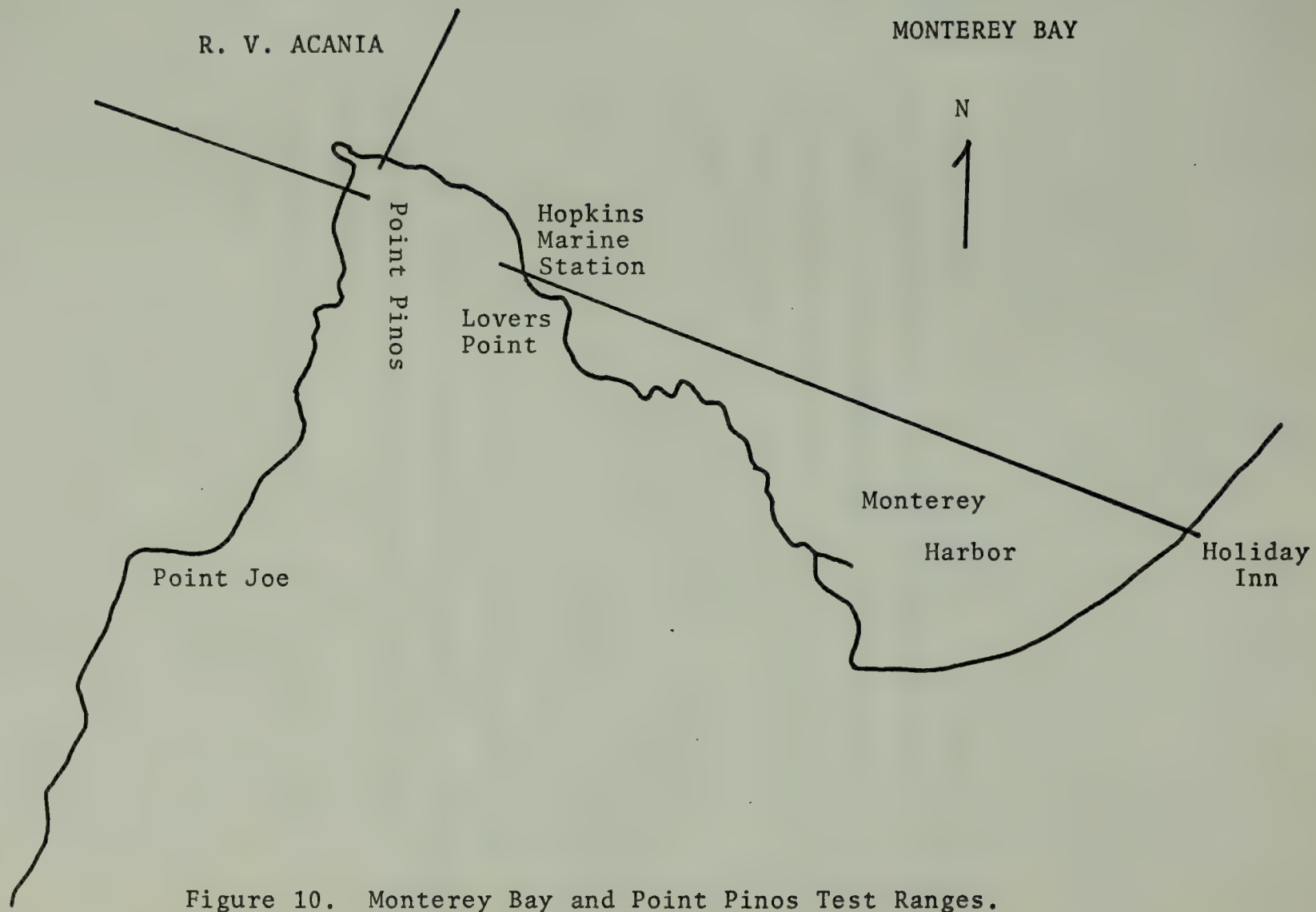

Figure 10. Monterey Bay and Point Pinos Test Ranges.

IV. EXPERIMENTS

The previous measurements of beam wander and spread over water were conducted by Beal. He conducted five experiments, three of which he classified as successful. Significantly the three successful trials were conducted with both laser source and telescope ashore. The propagation path was approximately 4km over the southern end of Monterey Bay. The other two experiments were conducted with the source onboard the R. V. ACANIA and the telescope ashore.

The scanning telescope is very sensitive to angular stability but is relatively insensitive to source intensity. This virtually precludes mounting the telescope on anything other than a stable foundation. On the other hand, scintillation detectors are less sensitive to detector angle fluctuations but are critically sensitive to intensity fluctuations. This precludes mounting the scintillation source on other than a stable platform.

Due to the above considerations, ship to shore experiments are currently conducted with the gyro-stabilized source located on board the R. V. ACANIA and the scanning telescope located ashore. The laser which is mounted on the telescope tó provide a signal for the gyro tracking circuitry also acts as the source for the scintilometers. The scintilometers are mounted on the gyro and are kept aligned by the gyro.

Although the laser source is gyro-stabilized, there are still many significant motion problems to be dealt with. The ship on which the source is mounted moves vertically and to a lesser extent horizontally both along the propagation path and perpendicular to it. At the same time it rolls and pitches. In trying to compensate for the three translational and two rotational motions the gyro superimposes its own motion on the beam. In tracking the moving source the telescope adds yet another motion to the problem.

If the source were located ashore, all of the above motions would be eliminated and the only motion of the beam would be that which resulted from atmospheric effects. However, if both source and telescope were placed ashore, then the propagation path would include two overland portions and two ocean-land interfaces. These areas would have considerable effect on the propagation of the beam which would not be reflected in the micrometeorological measurements taken over the water. Because the purpose of the experiment was to measure the atmospheric effects over water, it was decided not to place the source ashore but to deal with the problems caused by the moving source. Considerable progress has been made on the solutions to these problems.

The two source lasers are mounted on a gyro-stabilized platform in such a manner that their beams propagate parallel to the gyro axis. The platform locks on to and tracks a 6328 Å signal from the telescope. The tracking device is a quadrant photocell with circuitry to form differences between

the right and left quadrant signals and up and down quadrant signals. It combines these with the perpendicular derivatives to generate the error signals which drive the torque motors that eliminate the tracking errors. The circuitry incorporates automatic gain control so that tracking is independent of intensity.

The telescope is mounted inside a portable trailer with its foundation extending through the trailer floor to the ground. The trailer portects the telescope, associated equipment, and operators from the elements without interfering with its solid foundation. The telescope is now equipped with two manually operated screw actuated slide translators for tracking in both train and elevation. This requires a full time operator but has proved effective in moderate seas.

Data is recorded continuously while the gyro tracks the telescope. After the experiment is concluded, the tapes are reviewed and short sections of tapes which appear to have stable signals are identified for data processing. The fast Fourier transform methods employed require only a few seconds of stable signals.

A. EARLY EXPERIMENTS

An experiment was conducted with the source on board the R. V. ACANIA in the southern end of Monterey Bay on the seventeenth of January. The telescope was mounted in a van at Hopkins Marine Station. Another experiment was conducted

with the ACANIA in open water off Point Pinos on the twenty-fifth and twenty-seventh of February. The trailer was first used to transport and protect the telescope during this experiment. A small portable generator provided power. Another experiment was conducted off Point Pinos on the sixth of March. None of these experiments yielded reducable data but all yielded significant information for further development of apparatus and procedures. Two other experiments were conducted off Point Pinos in March. These also yielded small amounts of reducable data.

B. LATER EXPERIMENTS

1. 7 June 1974

Following extensive modifications to the telescope scanning and detector units which gave the telescope an infrared as well as a visible capability, an experiment was conducted on the roof of Spanagel Hall on the seventh of June. The sources were a 10.6μ CO_2 laser and a 6328 Å He-Ne laser, mounted in the same vertical plane with the CO_2 laser 20 cm above the He-Ne. The He-Ne laser was bore sighted to the CO_2 laser. The system worked well but several unexpected effects were noted. First, a diffraction pattern was observed on the 10.6μ signal while none was noted on the 6328 Å signal. This was caused by the vertical bar that holds the 45 degree turning mirror in place. The bar and telescope sides formed a two slit diffraction grating. The effect was not noted on the He-Ne signal because the telescope was not diffraction limited at that wavelength.

An attempt was made to eliminate the diffraction pattern by rotating the scan direction 90 degrees. The scan was shifted from horizontally across the bar to vertically along the bar. This resulted in the loss of the CO_2 signal. Investigation revealed that the CO_2 signal was not lost but displaced approximately one miliradian from the He-Ne signal due to the 20 cm vertical separation of the two lasers. The effect had not been noted when scanning horizontally because the two lasers were located in the same vertical plane.

Data were recorded but the signals showed excessive scintillation due to turbulence and temperature gradients on the roof. More meaningful data could have been recorded in the less turbulent basement corridor but safety considerations precluded radiating the CO_2 laser in this area.

2. 10 June 1974

A more meaningful test was conducted with the two sources located at Hopkins Marine Station and the telescope at the Holiday Inn. The propagation path was approximately 4.3 km long, 10m above the waters of Monterey Bay. The telescope scanned vertically to minimize the diffraction of the 10.6 signal. At 4.3 km the two sources were only 0.05 miliradians apart. This angular separation was barely noticeable and did not create any problems.

3. 13 June 1974

Following the experiment of 10 June 1974, the scanner unit was relocated so that the bar holding the 45 degree

bending mirror would be horizontal instead of vertical. This was accomplished so that the scanner could scan horizontally and vertical motion of the source on board the ACANIA would be along the slit instead of superimposed on the scan.

Minor difficulties were encountered during the experiment. The primary one was caused by the dewar flask sweating and disrupting the 10.6 signal. However, significant amounts of useful data were recorded.

V. DATA REDUCTION

Data were reduced by fast Fourier transform methods utilizing a 1923 Time Series System. Although the system has many more capabilities, it was used to take direct Fourier transforms, inverse Fourier transforms, and to average.

Figures 11, 12, 13, and 14 are taken from 6328 Å data recorded during the experiment of June tenth. The propagation path was 4km over water from Hopkins Marine Station to the Holiday Inn. Scan was 10 volts at 25Hz. The slit width setting was 5.5 Figure 11 is the waveform average of 256 peaks. Figure 12 is the Fourier transform of that average waveform. Figure 13 is the average Fourier transform of 128 peaks during the same time frame. Figure 14 is the inverse Fourier transform of Figure 13. Figure 15 is the waveform average of 256 10.6 peaks recorded at the same time with the same setting. Figure 16 is the average Fourier transform of 256 peaks during the same period. Figure 17 is the inverse Fourier transform of Figure 16.

Figure 18 is the Fourier transform of an idealized signal obtained by creating a parallel beam with a 10 inch mirror identical to the telescope primary mirror. The mirror was located directly in front of and as close to the telescope as possible, thus minimizing atmospheric effects. Figure 18 is taken to be the MTF of the telescope at the same

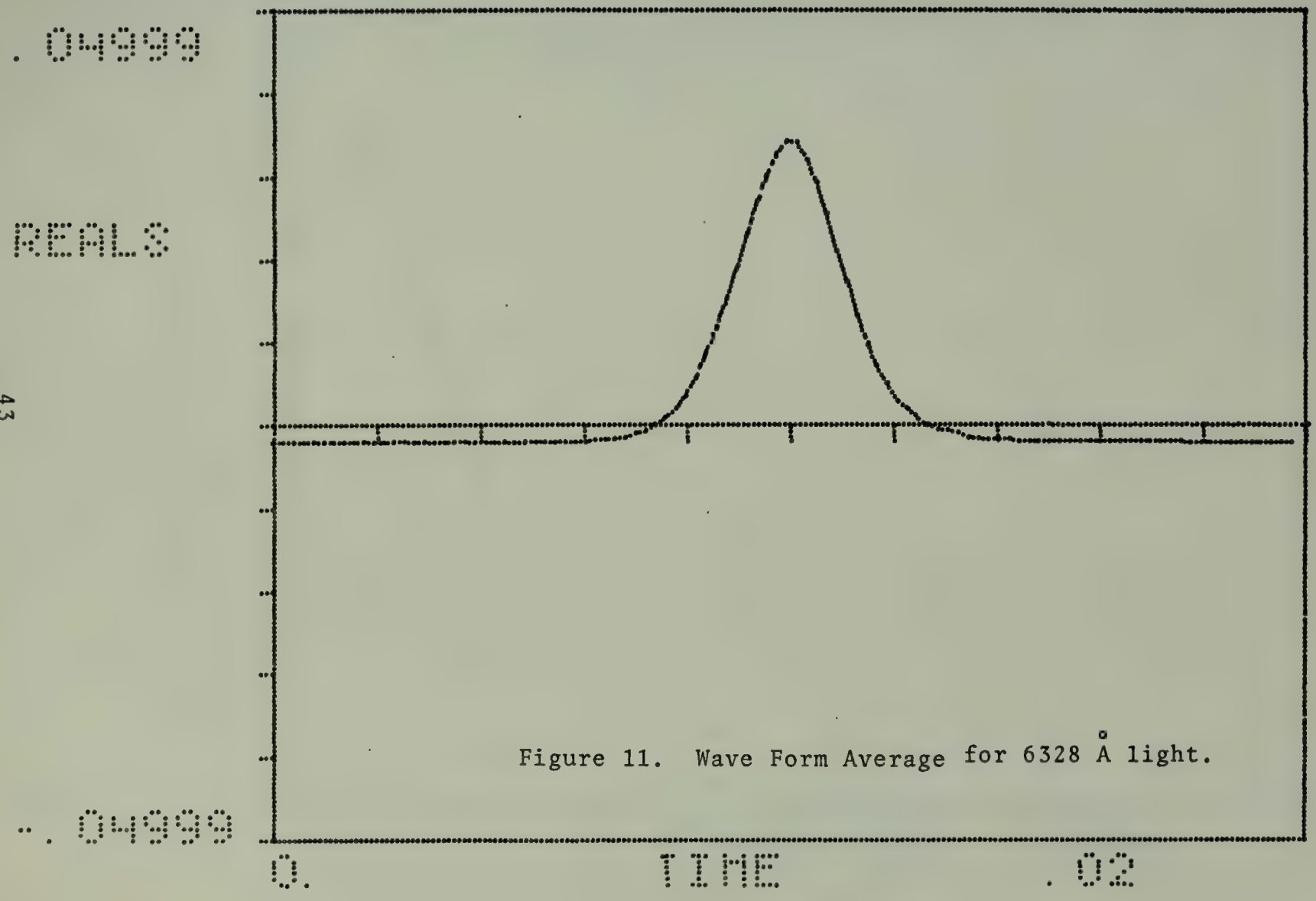

Figure 11. Wave Form Average for 6328 Å light.

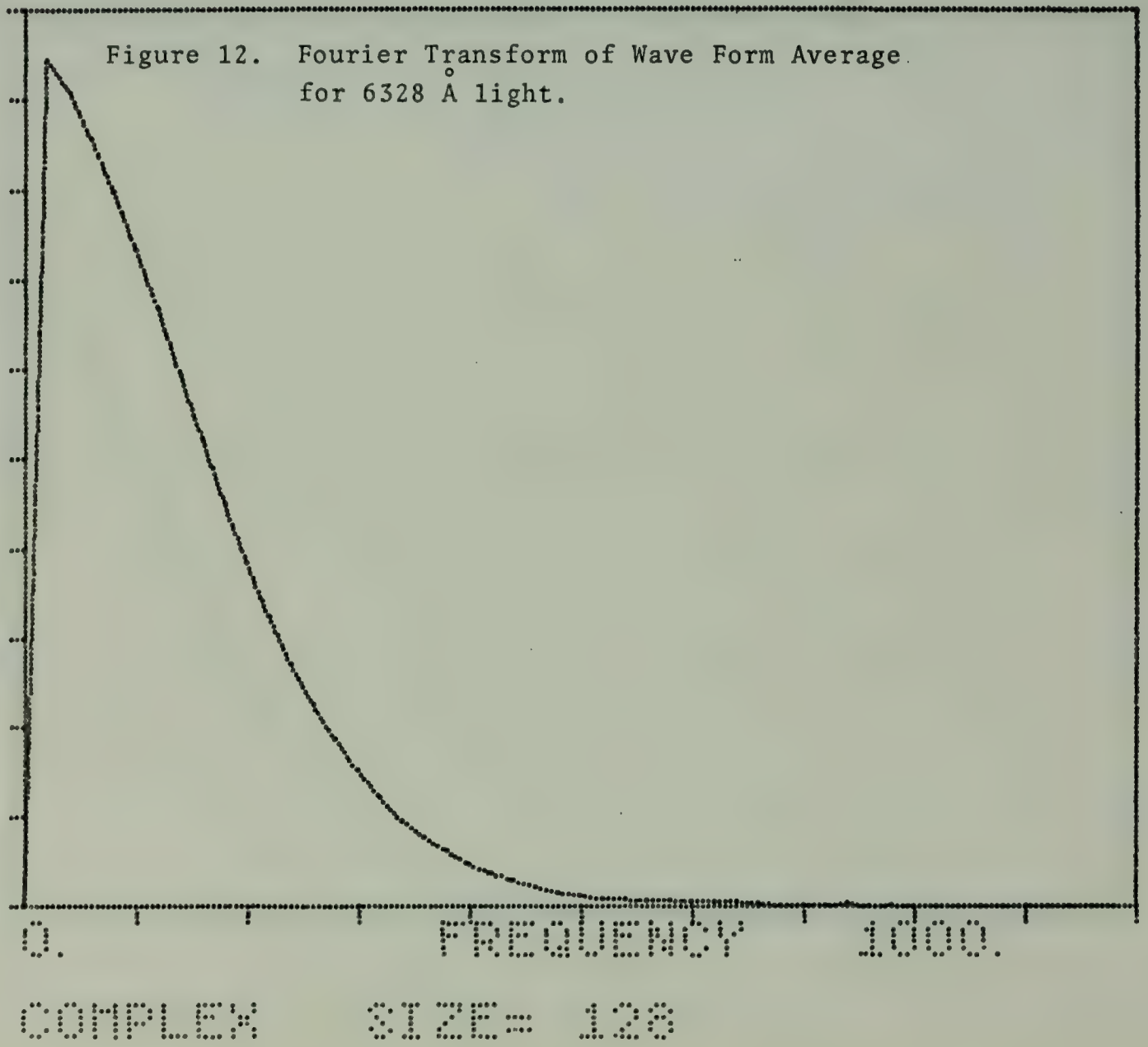

Figure 12. Fourier Transform of Wave Form Average for 6328 Å light.

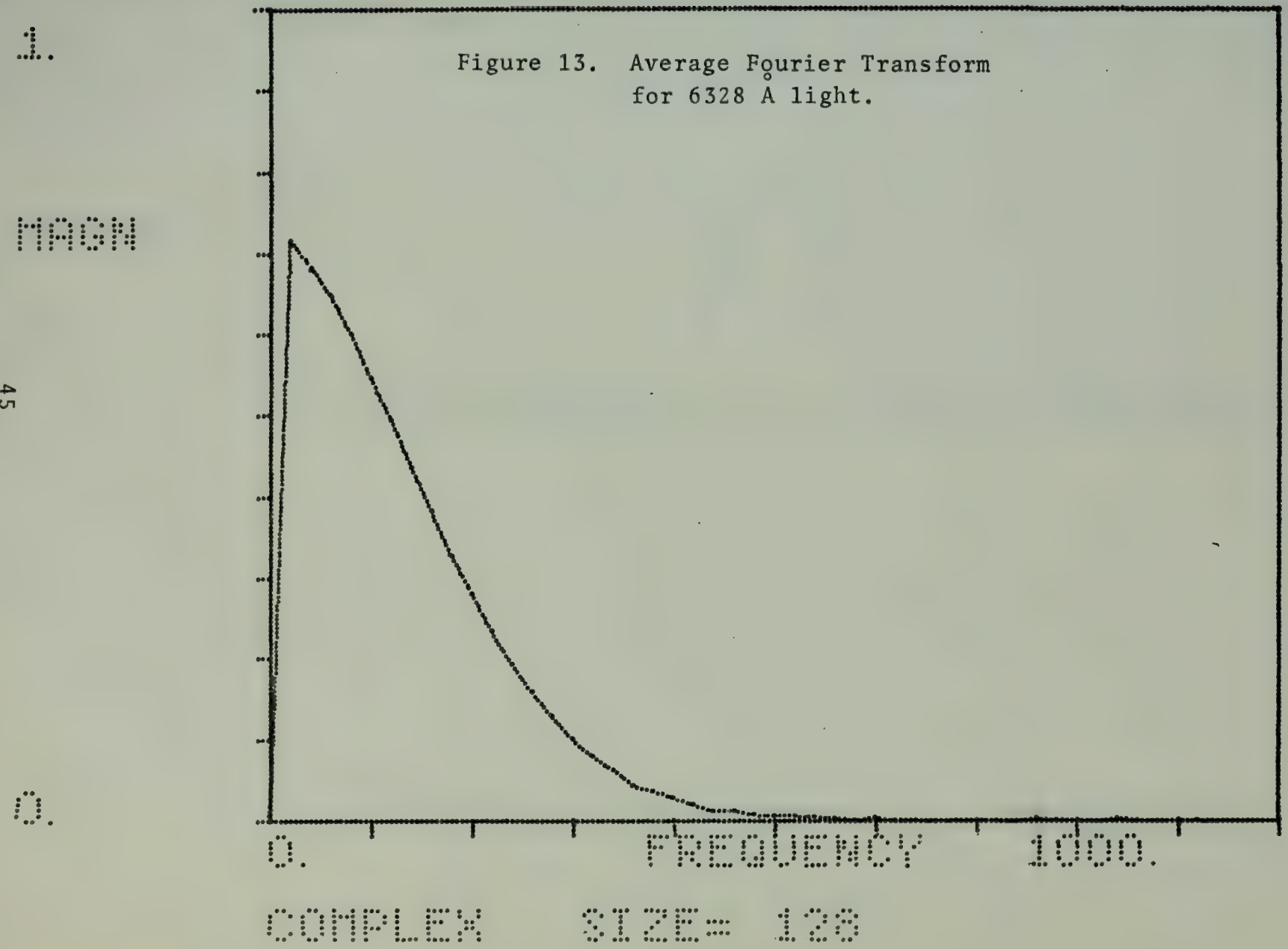

Figure 13. Average Fourier Transform for 6328 Å light.

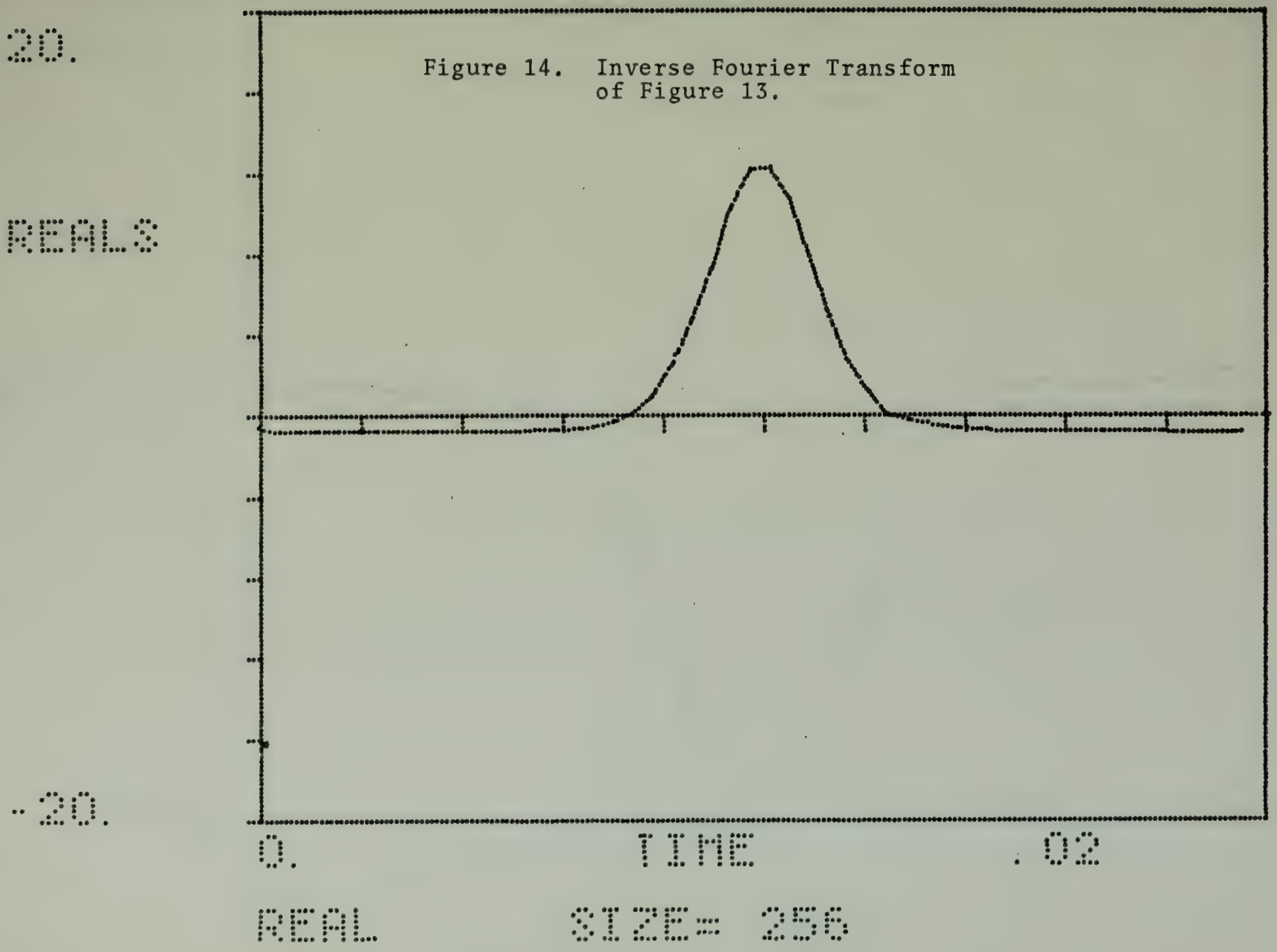

Figure 14. Inverse Fourier Transform of Figure 13.

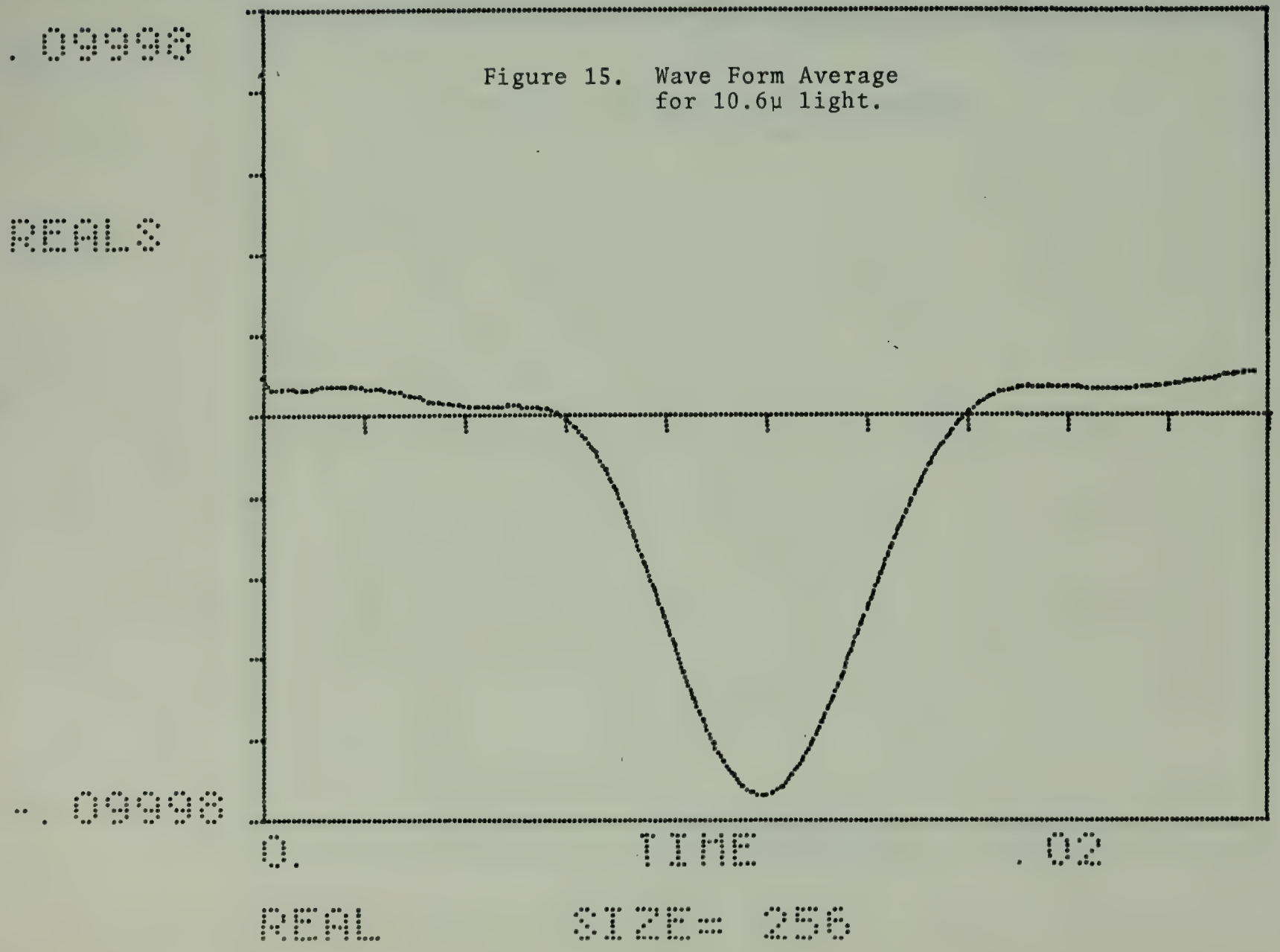

Figure 15. Wave Form Average
for 10.6μ light.

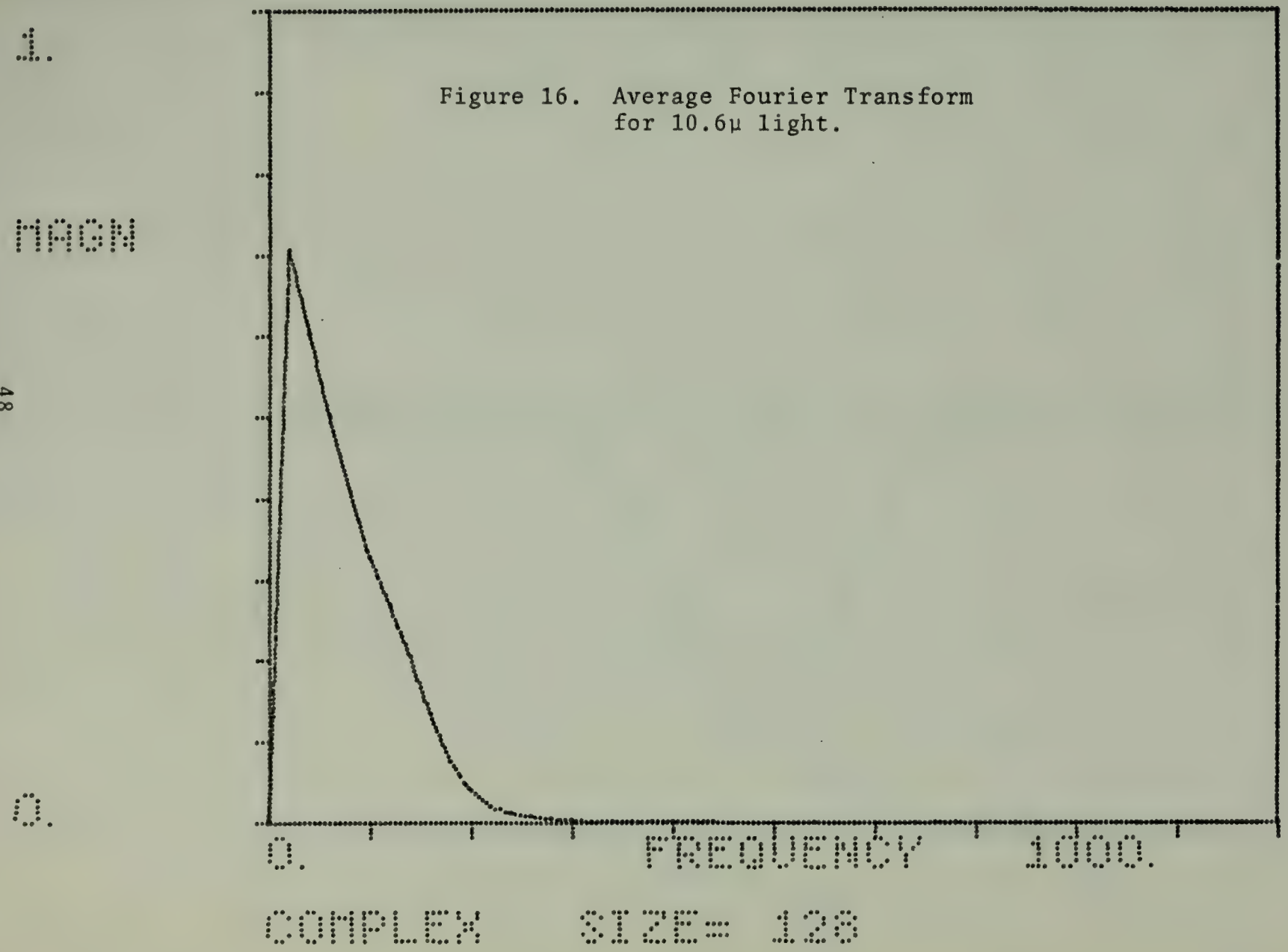

Figure 16. Average Fourier Transform for 10.6μ light.

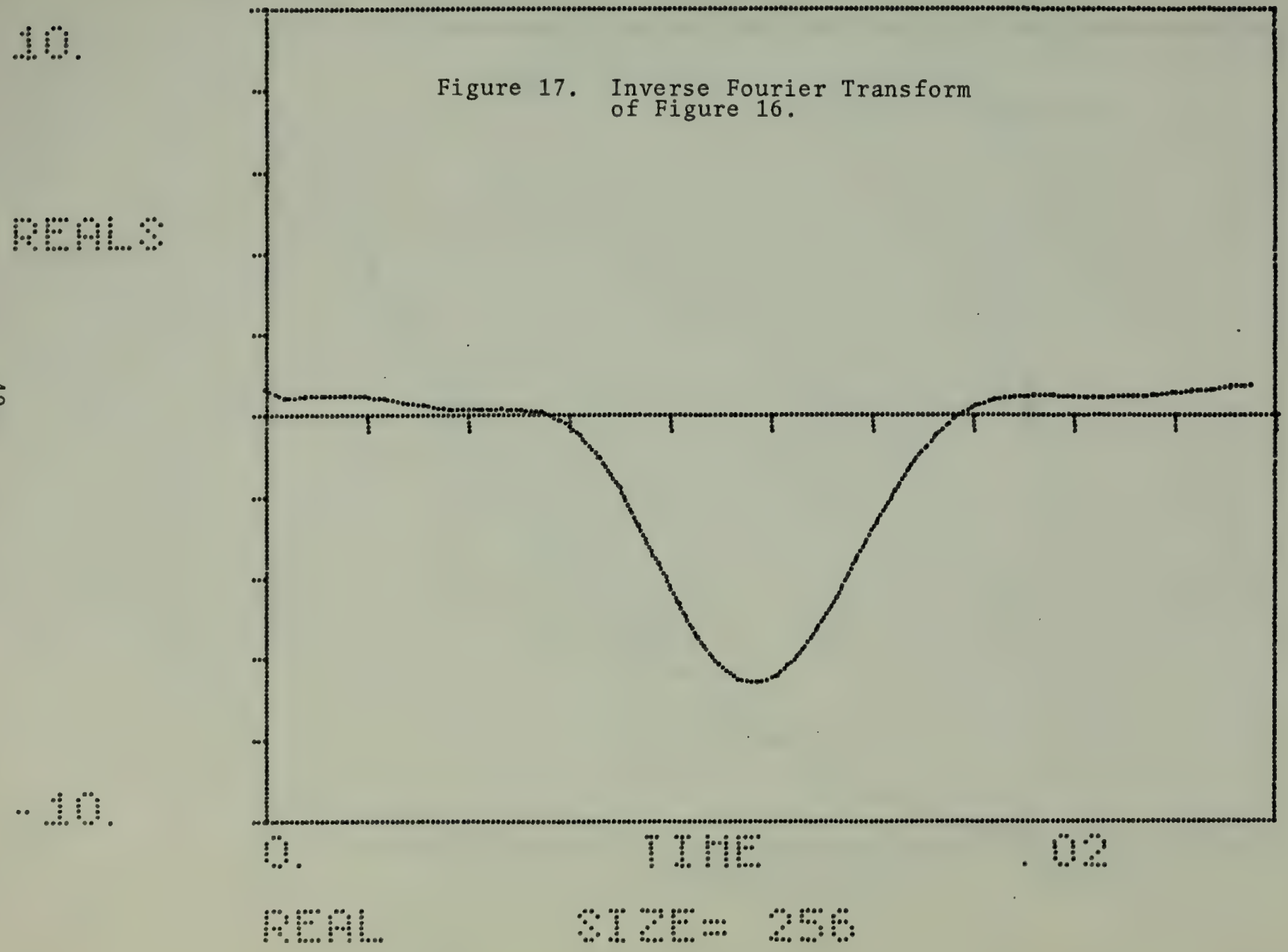

Figure 17. Inverse Fourier Transform of Figure 16.

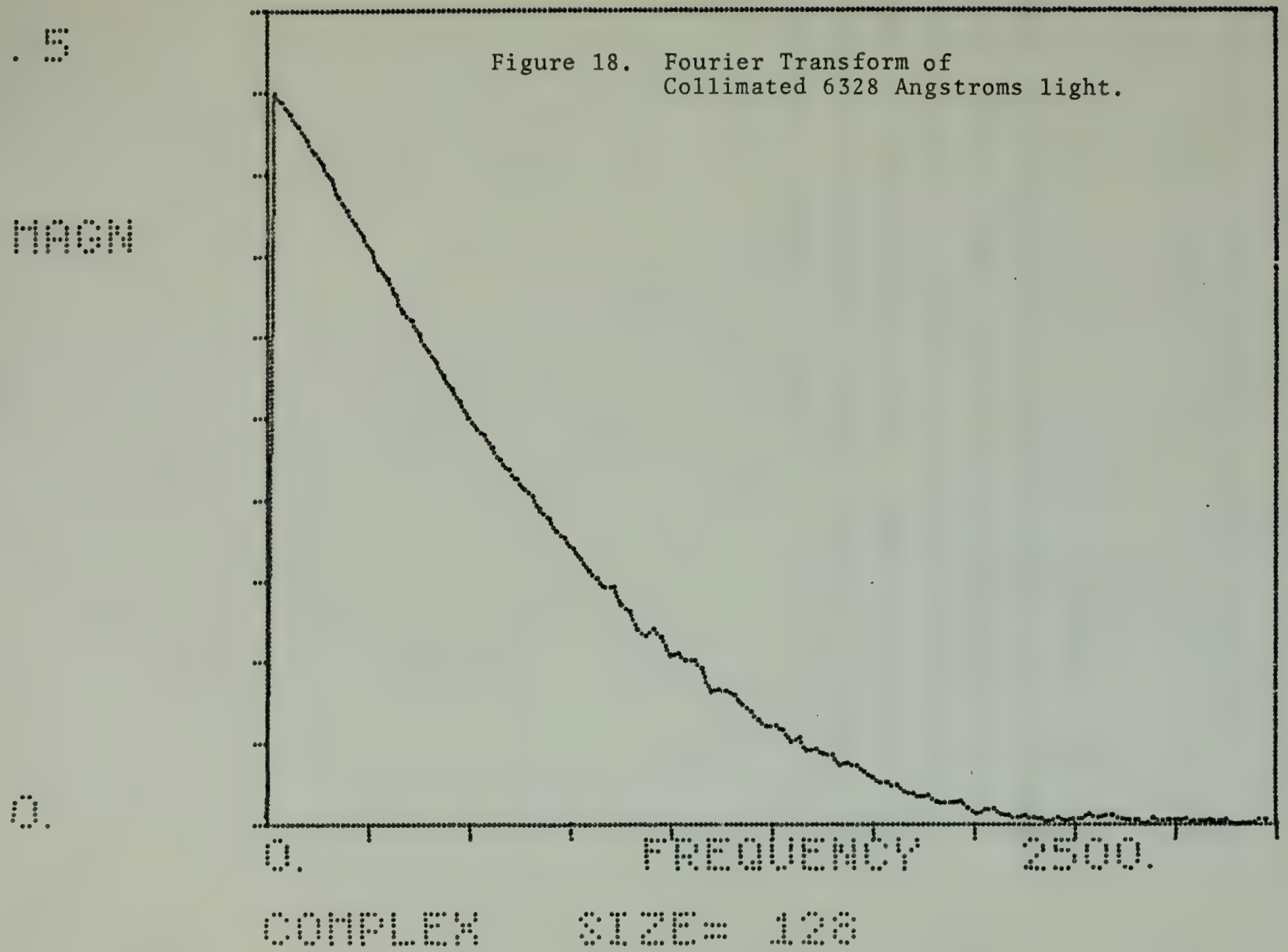

Figure 18. Fourier Transform of
Collimated 6328 Angstroms light.

setting used above. Figure 19 is the inverse Fourier transform of Figure 18. The MTF of the atmosphere, Figure 20, for 6328 Å radiation was obtained by dividing the absolute values of the values of Figure 12 by those of Figure 18 point by point.

Figures 21, 22, 23, 24, and 25 also represent 6328 Å data recorded during the experiment of June tenth with the same settings, except that the diffraction grating is in place. Figure 21 is the average Fourier transform and Figure 22 its inverse transform. Figure 23 is the wave form average and Figure 24 its Fourier transform. Figure 25 is the inverse transform of Figure 24.

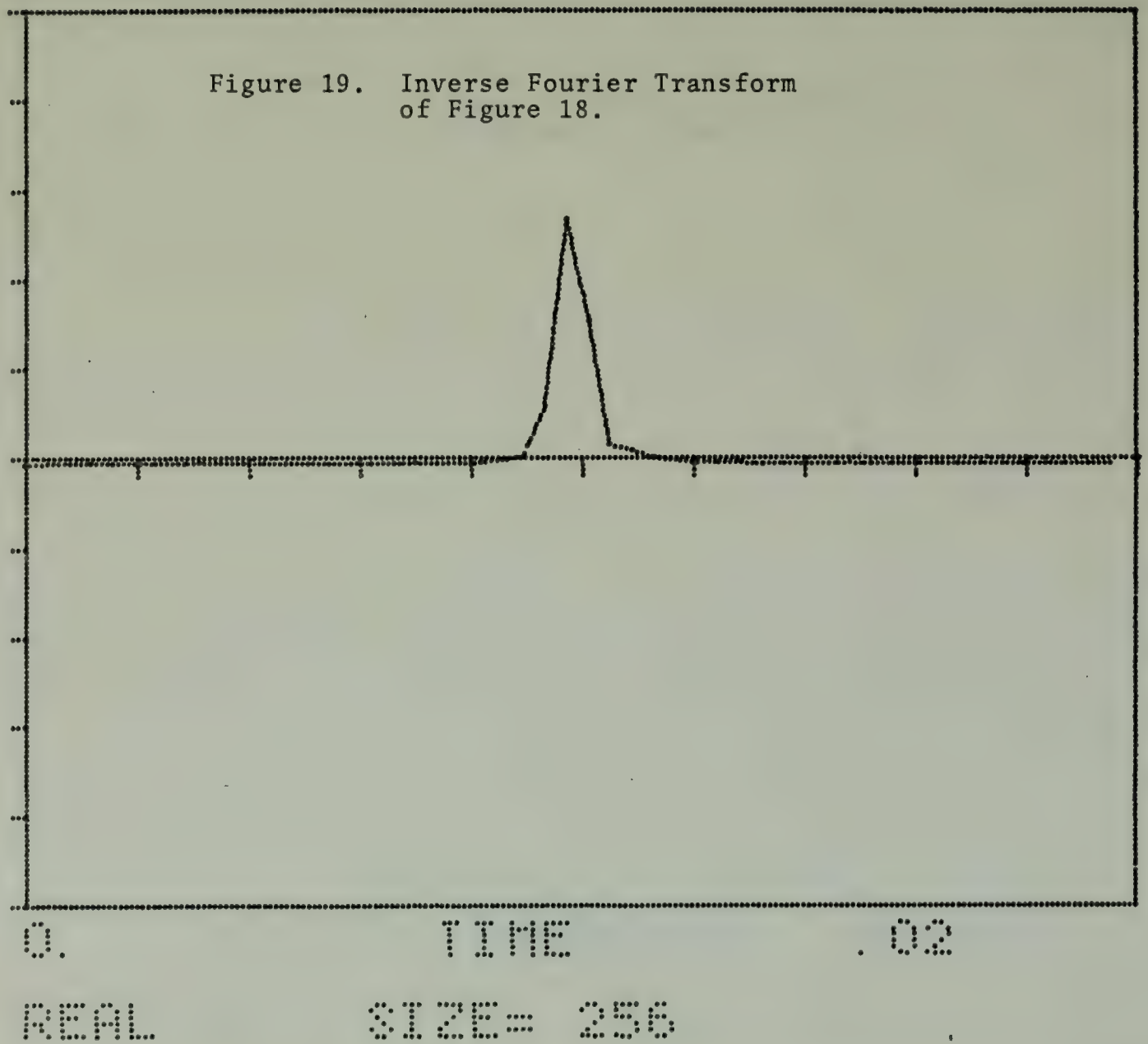

Figure 19. Inverse Fourier Transform of Figure 18.

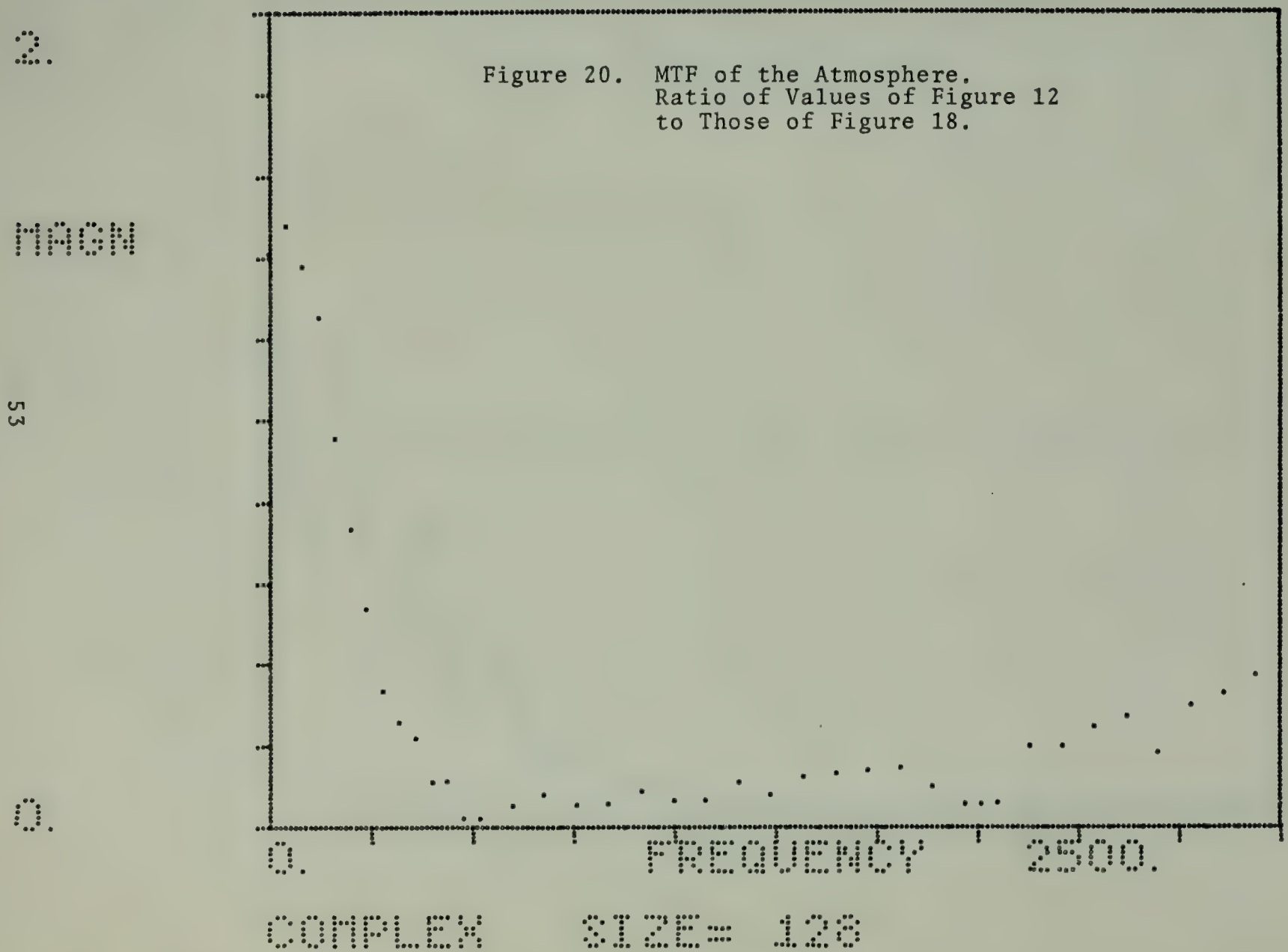

Figure 20. MTF of the Atmosphere. Ratio of Values of Figure 12 to Those of Figure 18.

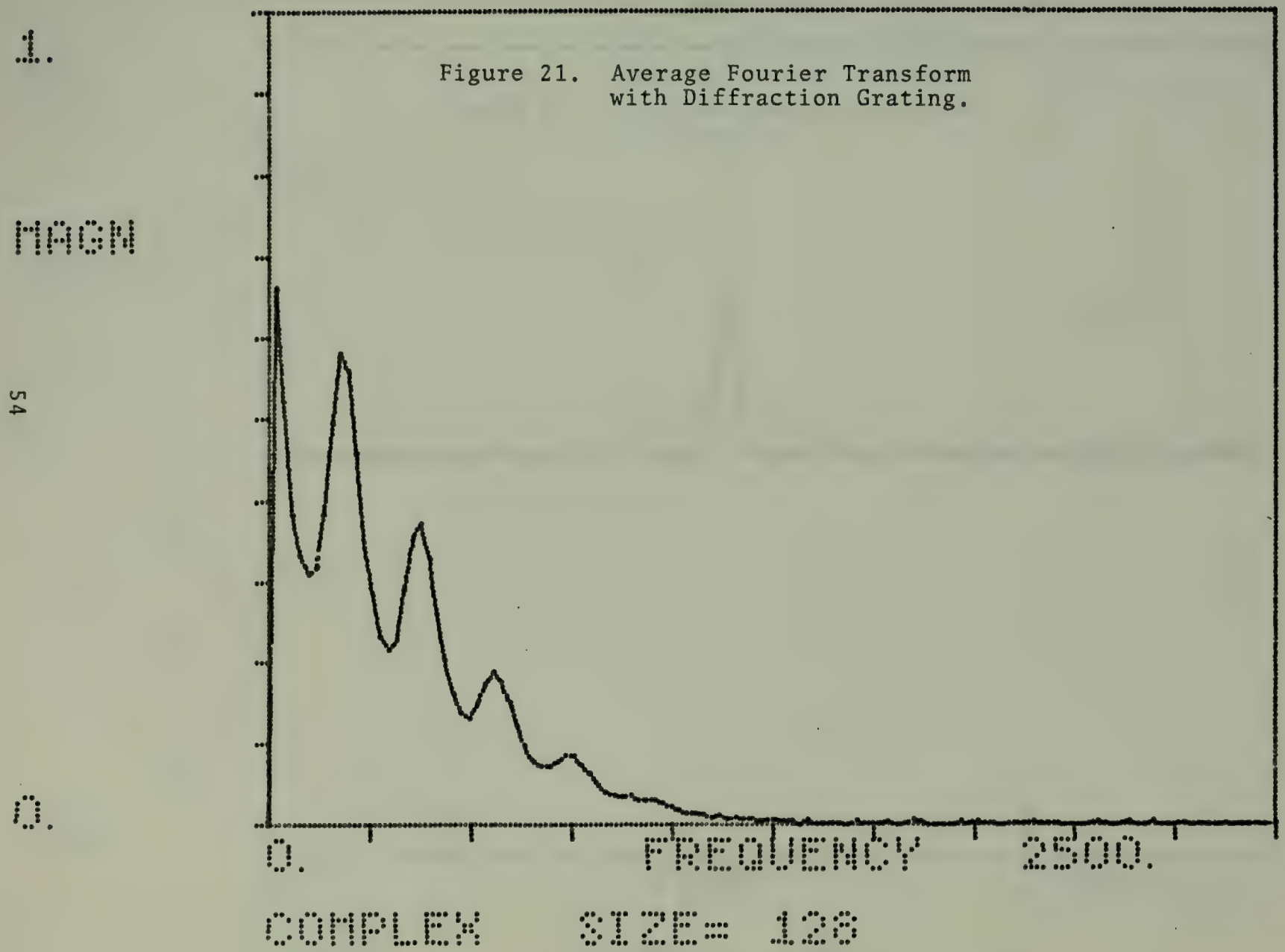

Figure 21. Average Fourier Transform with Diffraction Grating.

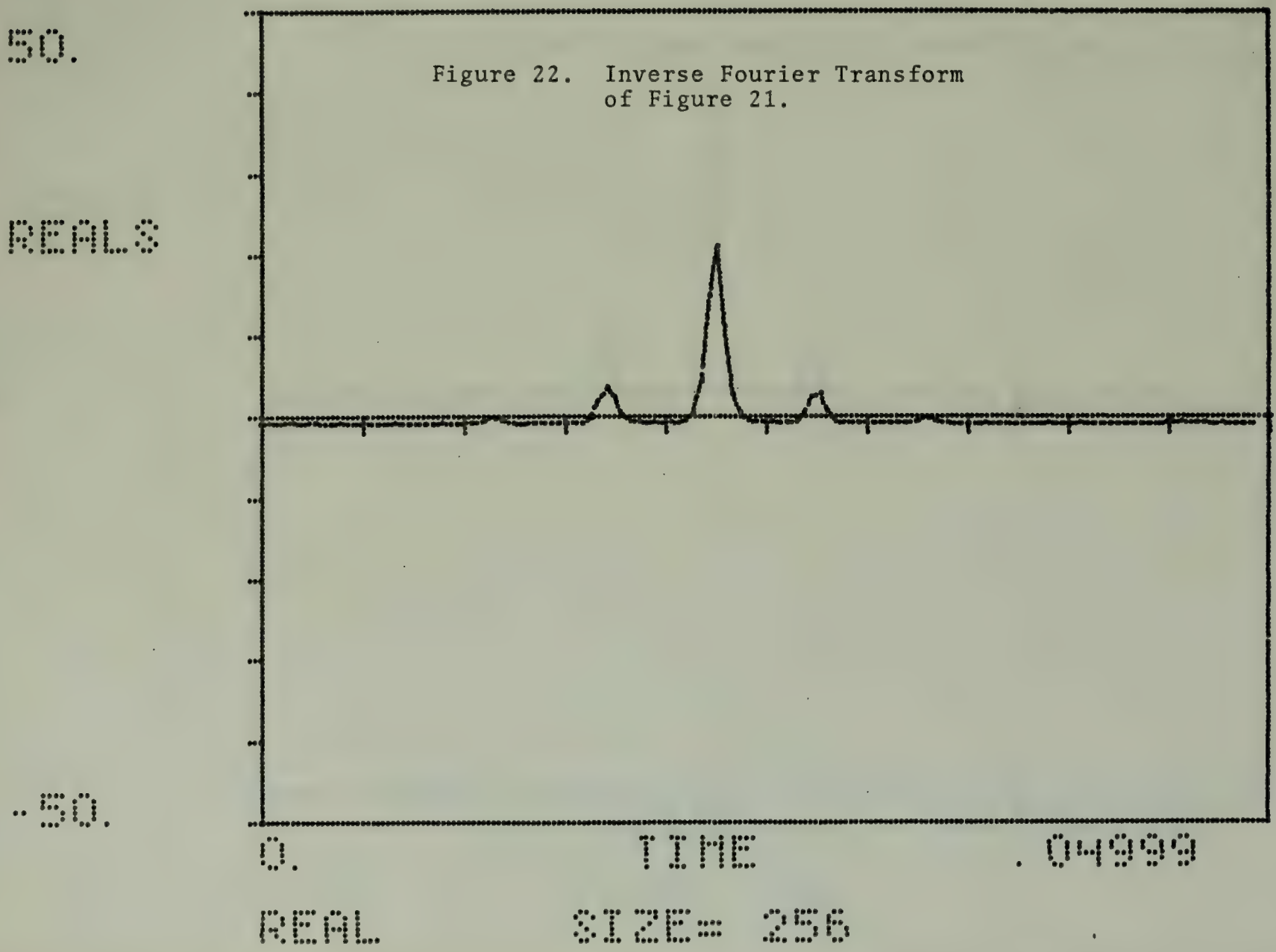

Figure 22. Inverse Fourier Transform of Figure 21.

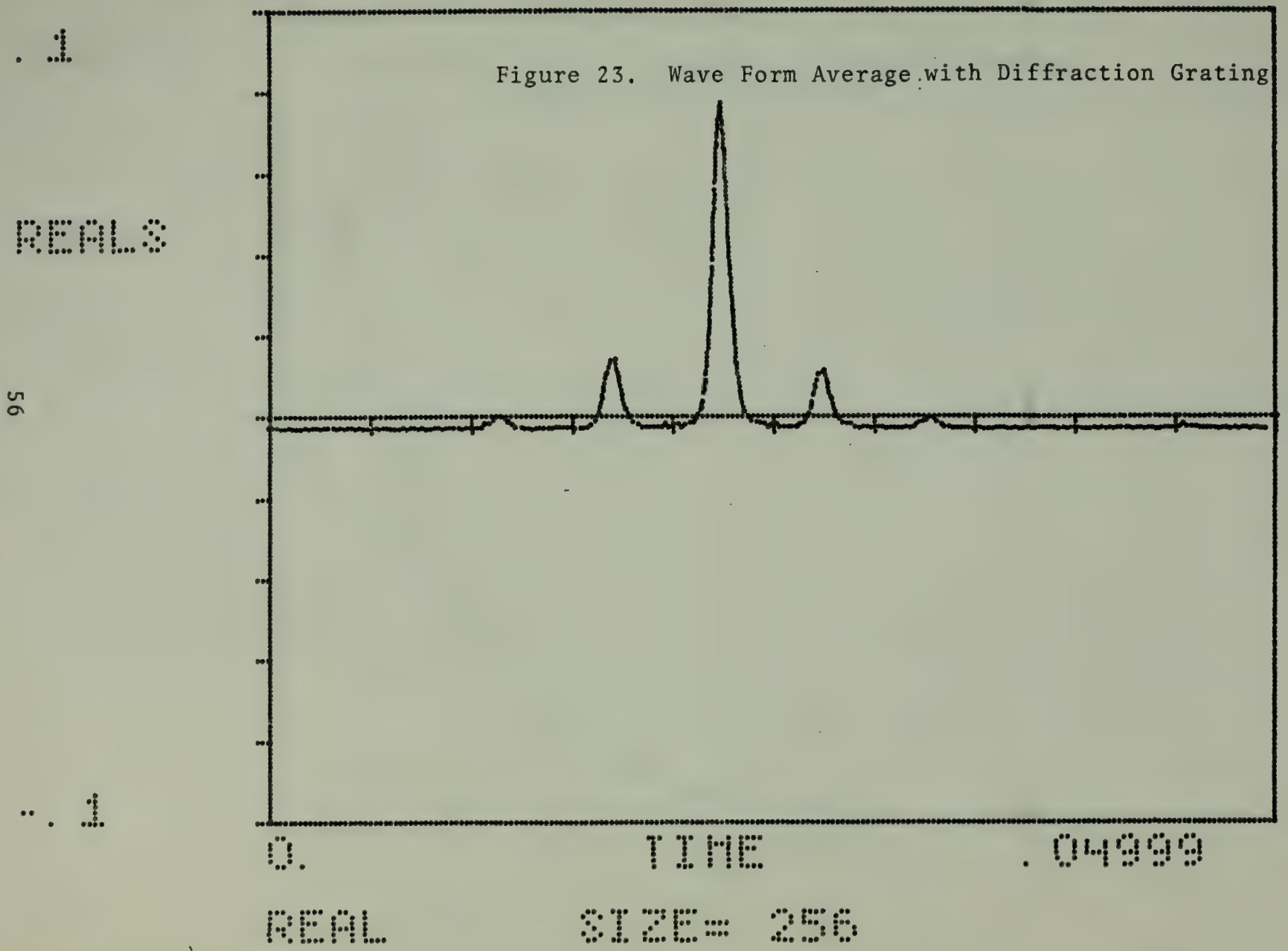

Figure 23. Wave Form Average with Diffraction Grating

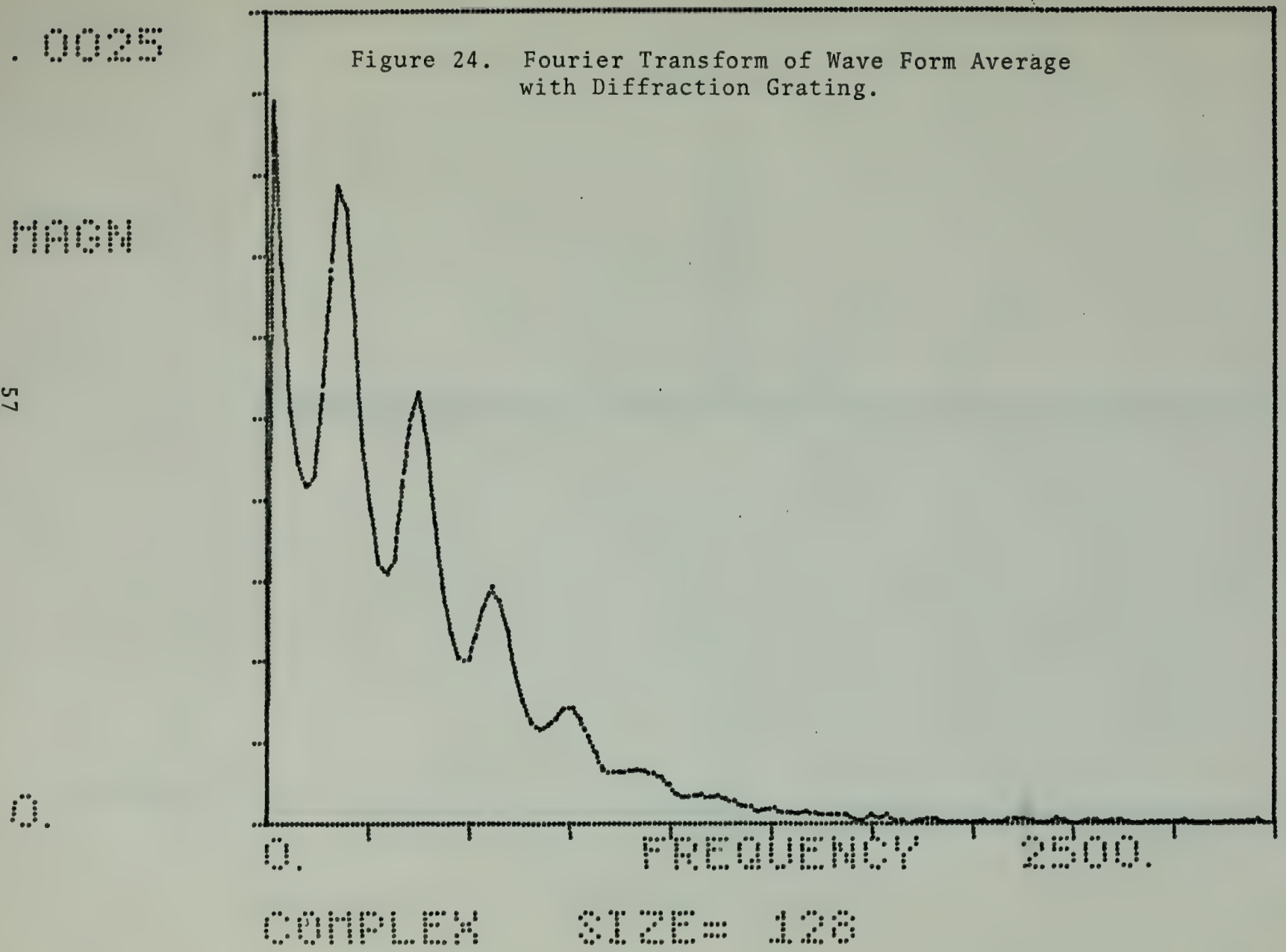

Figure 24. Fourier Transform of Wave Form Average with Diffraction Grating.

Figure 25. Inverse Fourier Transform
of Figure 24.

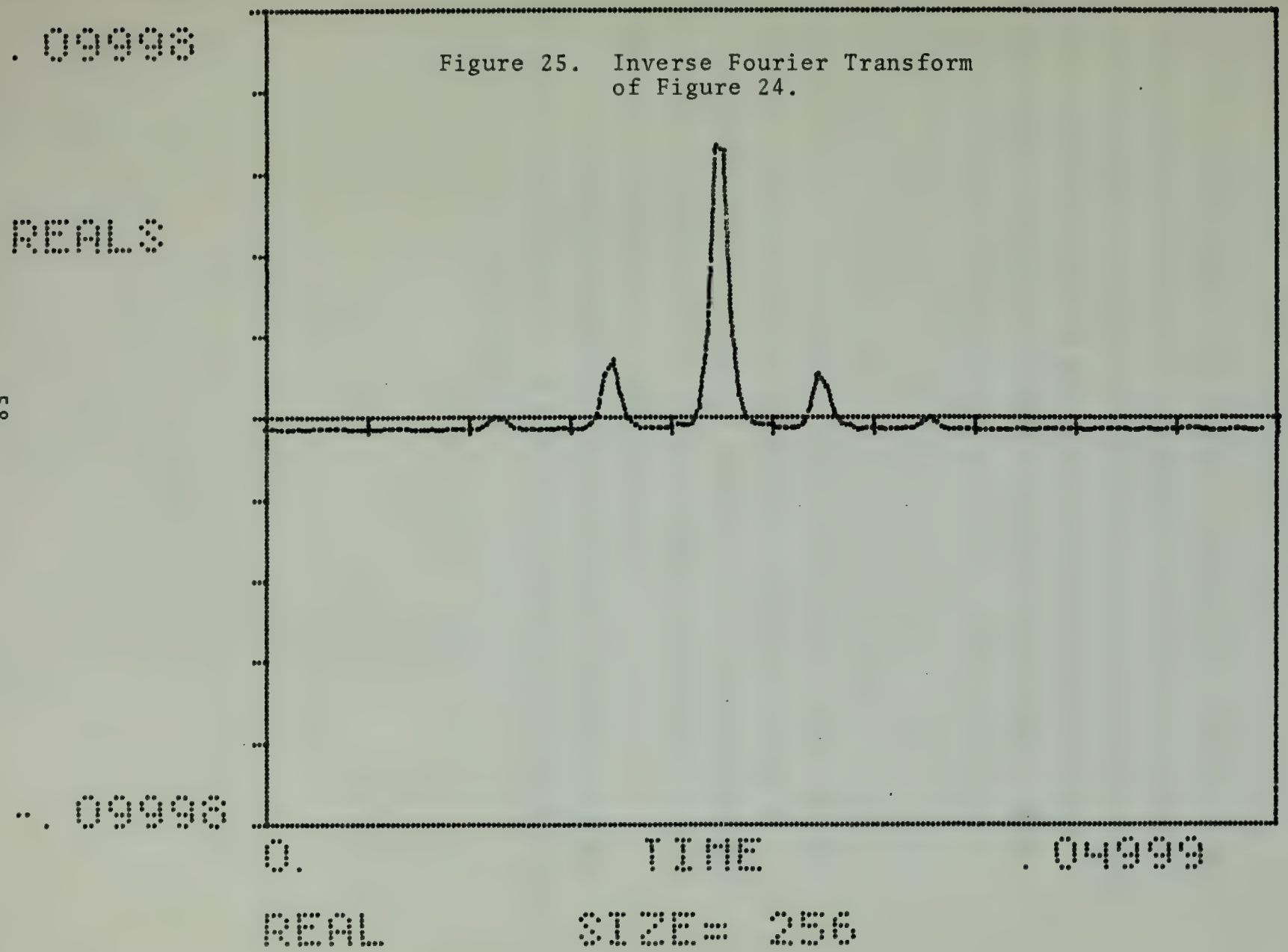

VI. CONCLUSIONS

The system described is still in the evolutionary stage. As currently configured it has been successfully operated to obtain the MTF of the atmosphere for a 6328 Å laser beam. Further development of the apparatus is already underway. An 18 inch primary mirror has already been obtained. With it, the telescope will be reconfigured, thereby reducing diffraction effects at the longer wavelengths. After the telescope is reconfigured, it will be necessary to measure the MTF of the telescope at 6328 Å and 10.6μ so that the MTF of the atmosphere can be determined at those wavelengths. Plans have also been made to linearize the scanning mirror movement by adding higher order Fourier components to the present sinusoidal scan drive signal.

It is recommended that the telescope be modified to add a capability to work at 3.8μ so that wavelength dependence may be studied in more detail.

COMPUTER PROGRAM MODFUN

June 16, 74

Displays the "Modulation Function" The Division of a perturbed function's Fourier transform magnitude by the magnitude of the transform for an ideal function

P0 = No. of frames of each function averaged
P1 = Caspec Gain

```
SAVE MODFUL
CREATE MODFUL
XREF ADIT
XREF AVFT
XREF CASPEC
XREF XSROOT
XREF DISPLY
10 BLKCLR
20 BLKDEF B0,256,1,0
30 ZERO B0
40 BLKDEF B1,256,1,256
50 ZERO B1
60 BLKDEF B3,512,1,512
70 ZERO B3
80 BLKDEF B4,256,1,1024
90 ANINIT B0,256,1,7,1,55,1,2
100 FOR 10,1,P0
110 ANINP
115 DFT B0
120 RDIT B0,B3
130 NEXT 10
140 ANINIT
150 AVFT B3,B4,256
160 OSPEC 'CR'
170 BIBSET B4,0,5120
180 BIBSET B4,2,0
190 HINPUT 11,'G'
200 BLKDEF B5,256,1
210 BLKDEF B6,256,1
220 ZERO B5
230 ZERO B6
240 BLKDEF B7,512,1
250 ZERO B7
260 BLKDEF B8,128,3
270 ANINIT B5,256,1,7,1,55,1,2
280 FOR I2,1,P0
```

```
290 ANINP
300 DFT B5
310 ADIT B5,B7
320 NEXT 12
330 ANINIT
340 AVFT B7,B8,P0
350 DASPEC B4,P1,0,128
360 XSROOT B4,0,128
370 CASPEC B8,P1,0,128
380 XSROOT B8,0,128
385 BIBSET B4,0,5120
386 BIBSET B4,2,4
390 BIBSET B8,0,5120
400 BIBSET B8,2,4
410 OSPEC 'CP'
420 DISPLY B4, 'M' DEC,128,'G'
432 DISPLY B8, 'M' DEC,128,'G'
440 BLKDEF B9,128,2
450 FLORT B8,B9
486 OSPEC 'KB'
490 RETURN
END
```

COMPUTER PROGRAM AVSPEC

June 16,74

```
SAVE AVSPEC
CREATE AVSPEC
XREF ADIT
XREF AVET
XREF DISPLY
10 BLKCLR
20 BLKDEF B0,256,1,0
30 ZERO B0
40 BLKDEF B1,256,1,256
50 ZERO B1
60 BLKDEF B3,512,1,512
70 ZERO B3
80 BLKDEF B4,128,3,1024
90 ANINIT B0,256,1,7,1,55,1,2
100 FOR I0,1,P0
110 ANINF
120 DFT B0
130 ADIT B0,B3
140 NEXT I0
150 ANINIT
160 AVFT B3,B4,P0
170 BIBSET B4,0,5120
180 BIBSET B4,2,4
190 OSPEC 'CR'
200 DISPLY B4,'M','DEC',128,'G'
210 IFT B4
220 DISPLY B4,'RE','DEC',128,'G'
230 OSPEC 'KB'
240 RETURN
END
```

COMPUTER PROGRAM AVWAVE

June 16,74

P0 = NO OF FRAMES AVERAGED

```
>SAVE AVWAVE
CREATE AVWAVE
XREF ADIT
XREF AVFT
XREF DISPLY
10 BLKCLR
20 BLKDEF B0,256,1,0
30 ZERO B0
40 BLKDEF B1,256,1,256
50 ZERO B1
60 BLKDEF B3,512,1,512
70 ZERO B3
80 BLKDEF B4,256,1,1024
90 ANINIT B0,256,1,7,1,55,1,2
100 FOR I0,1,P0
110 ANINP
120 ADIT B0,B3
130 NEXT I0
140 ANINIT
150 AVFT B3,B4,256
160 OSPEC 'CR'
170 BIBSET B4,0,5120
180 BIBSET B4,2,0
190 DISPLY B4,'RE','DEC',256,'G'
200 DFT B4
210 BIBSET B4,0,5120
220 BIBSET B4,2,4
230 DISPLY B4,'M','DEC',128,'G'
240 IFT B4
250 DISPLY B4,'RE','DEC;,128,'G'
260 OSPEC 'KB'
270 RETURN
END
```

BIBLIOGRAPHY

1. U. S. Air Force, Handbook of Geophysics, The MacMillan Company, New York, 1960, pp. 13-20.

2. Tatarski, U. I., Wave Propagation in a Turbulent Medium, McGraw-Hill, 1961.

3. Hufnagel, R. E. and Stanley, N. R., "Modulation Transfer Function Associated with Image Transmission Through Turbulent Media," Journal of the Optical Society of America, Vol. 54, pp. 52-61, January 1964.

4. Beal, D. A., An Experiment to Measure Laser Beam Wander and Beam Spread in the Marine Boundary Layer Near Shore, MS Thesis, Naval Postgraduate School, Monterey, California, 1973.

5. Strohbehn, J. W., "Line-of-Sight Wave Propagation Through the Turbulent Atmosphere," Proceedings of the IEEE, Vol. 56, pp. 1301-1813, August 1968.

6. Haagensen, B. G., Laser Beam Scintillation in the Marine Boundary Layer, MS Thesis, Naval Postgraduate School, Monterey, California, 1972.

7. Shroeder, A. F., Laser Scintillation Properties in the Marine Boundary Layer, MS Thesis, Naval Postgraduate School, Monterey, California, 1973.

8. Dowling, J. A. and Livingston, P. M., "Behavior of Focused Beams in Atmospheric Turbulence: Measurements and Comments on the Theory," Journal of the Optical Society of America, Vol. 63, pp. 846-858, July 1973.

9. Varvatsis, A. D. and Sancer, M. I., "Expansion of a Focused Laser Beam," Canadian Journal of Physcis, Vol. 49, pp. 1233-1247, May 1971.

10. Chiba, T., "Spot Dancing of the Laser Beam Propagated Through the Turbulent Atmosphere," Applied Optics, V. 10, pp. 2456-2461, 1971.

11. Fried, D. C., "Resolution Through Random Inhomogeneous Medium," Journal of the Optical Society of America, Vol. 56, pp. 1372-1379, October 1966.

12. Hildebrald, W. T., An Optical Apparatus to Determine The Effect of Turbulence on the Modulation Transfer Function of the Atmosphere, MS Thesis, Naval Postgraduate School, Monterey, California, 1967.

INITIAL DISTRIBUTION LIST

		No. Copies
1.	Defense Documentation Center Cameron Station Alexandria, Virginia 22314	2
2.	Library, Code 0212 Naval Postgraduate School Monterey, California 93940	2
3.	Professor O. Heinz, Chairman, Code 61Hz Department of Physics and Chemistry Naval Postgraduate School Monterey, California 93940	1
4.	Professor E. C. Crittenden, Jr., Code 61Ct Department of Physics and Chemistry Naval Postgraduate School Monterey, California 93940	8
5.	Professor E. A. Milne, Code 61Mn Department of Physics and Chemistry Naval Postgraduate School Monterey, California 93940	1
6.	LCDR Marion R. Alexander, Jr., USN 1124 Biak Avenue Armed Force Staff College Norfolk, Virginia	1

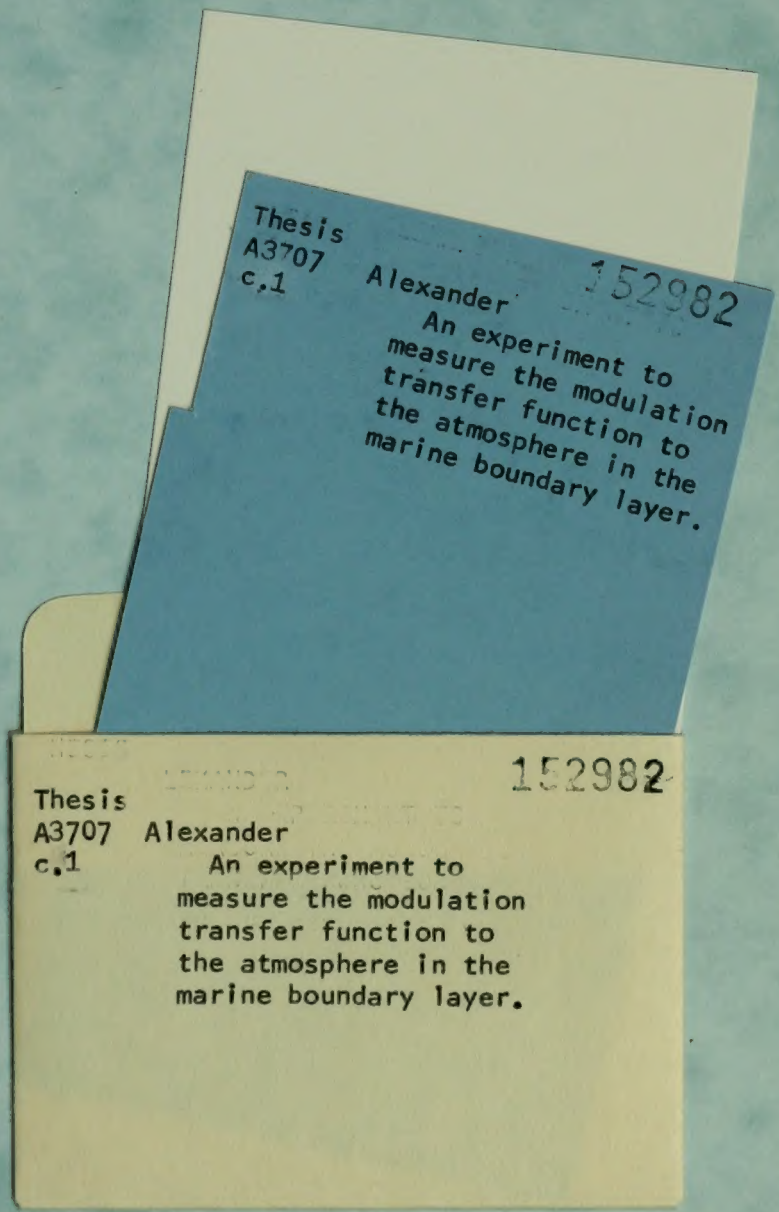
Thesis
A3707
c.1
Alexander
An experiment to measure the modulation transfer function to the atmosphere in the marine boundary layer.
152982
Thesis
A3707
c.1
Alexander
An experiment to measure the modulation transfer function to the atmosphere in the marine boundary layer.
152982